Konstantin Postnov
Sternberg Astronomical Institute, Moscow U.

Gravitational wave astronomy and its implications for cosmology

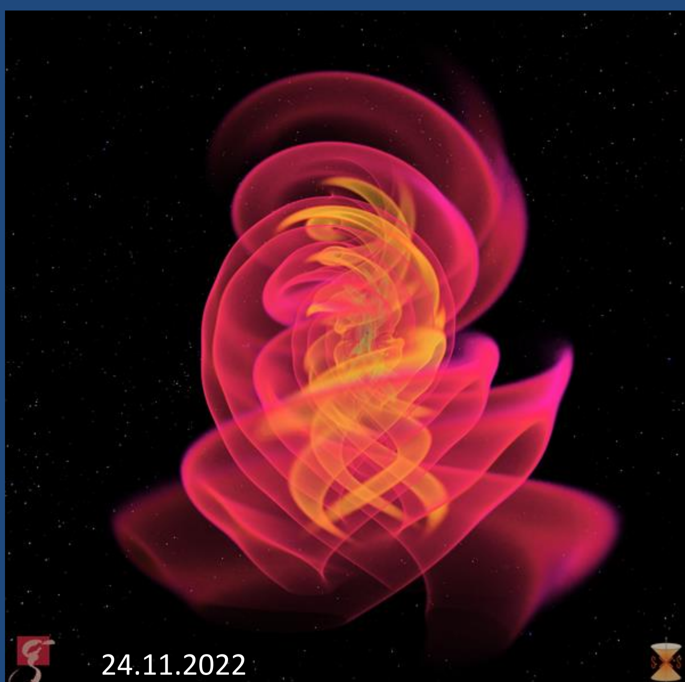

XXXIV International Workshop on High Energy Physics "From Quarks to Galaxies: Elucidating Dark Sides"

Plan

- Introduction
- 10-1000 Hz: ground-based laser interferometers
- LIGO/Virgo O1-O3
- Astrophysical implications
- NanoHz: pulsar timing arrays results

Gravitational waves

$$g_{\alpha\beta} = g^{\mathrm{B}}_{\alpha\beta} + h_{\alpha\beta} \ , \qquad R_{\alpha\beta\gamma\delta} = R^{\mathrm{B}}_{\alpha\beta\gamma\delta}$$

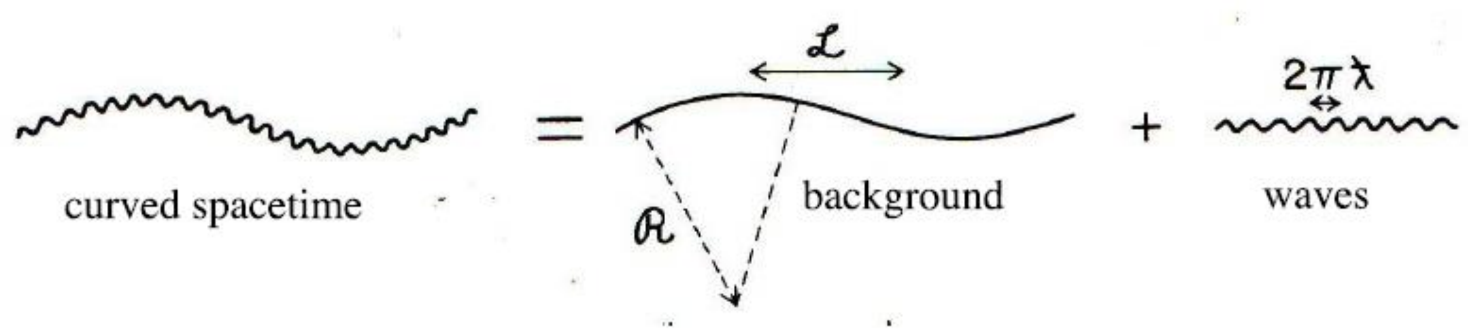

$$\Box \bar{h}_{\mu\nu} = -\frac{16\pi G}{c^4} T_{\mu\nu} \qquad \partial^{\nu} \bar{h}_{\mu\nu} = 0.$$

GW energy flux

- Energy density

$$t^{00} = \frac{c^2}{16\pi G}\langle \dot{h}_+^2 + \dot{h}_\times^2 \rangle$$

- Power

$$\frac{dE_{\mathrm{GW}}}{dt} = \frac{c^3 r^2}{16\pi G}\int d\Omega\, \langle \dot{h}_+^2 + \dot{h}_\times \rangle.$$

- Flux

$$T^{\mathrm{GW}\;0z} \simeq \frac{\pi}{4}\frac{c^3}{G} f^2 h_{\mathrm{amp}}^2 \simeq 300 \frac{\mathrm{ergs}}{\mathrm{cm}^2\ \mathrm{sec}} \left(\frac{f}{1\ \mathrm{kHz}}\right)^2 \left(\frac{h_{\mathrm{amp}}}{10^{-21}}\right)^2$$

GW emission

$$\bar{h}_{\mu\nu}(t,\mathbf{x}) = -4\frac{G}{c^2}\int_{\mathcal{V}} \frac{T_{\mu\nu}(t-|\mathbf{x}-\mathbf{x}'|/c,\mathbf{x}')}{|\mathbf{x}-\mathbf{x}'|} d^3\mathbf{x}'$$

- Quadrupole radiation for v/c<<1:

$$h_{jk}^{\mathrm{GW}} = 2G\frac{\ddot{I}_{jk}}{r} \sim G\frac{\omega^2(ML^2)}{r} \sim G\frac{E_{\mathrm{kin}}/c^2}{r}$$

$$\boxed{h_{jk}^{\mathrm{GW}} \sim h_+ \sim h_\times \sim 10^{-21}\left(\frac{E_{\mathrm{kin}}}{M_\odot c^2}\right)\left(\frac{100\mathrm{Mpc}}{r}\right)}$$

Astrophysical sources

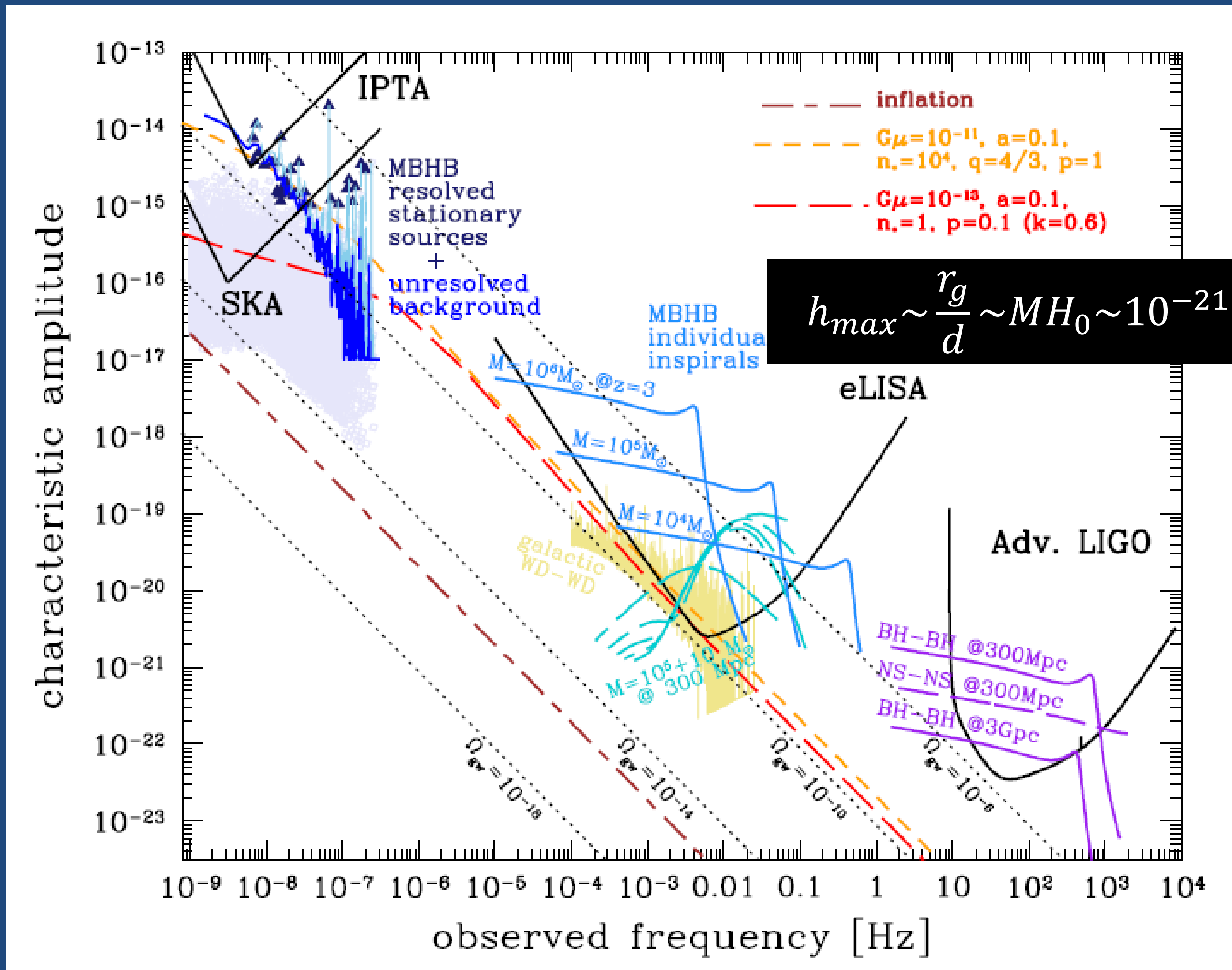

$$h_{max} \sim \frac{r_g}{d} \sim M H_0 \sim 10^{-21} \left(\frac{M}{10 M_o}\right)$$

GW produces tidal field

$$\boxed{\mathcal{E}_{ij} = R_{i0j0} = -\frac{1}{2}\ddot{h}_{ij}^{\mathrm{TT}}}$$

$$\boxed{h_{ij}^{\mathrm{TT}} \equiv -2\int dt \int dt\, \mathcal{E}_{ij}}$$

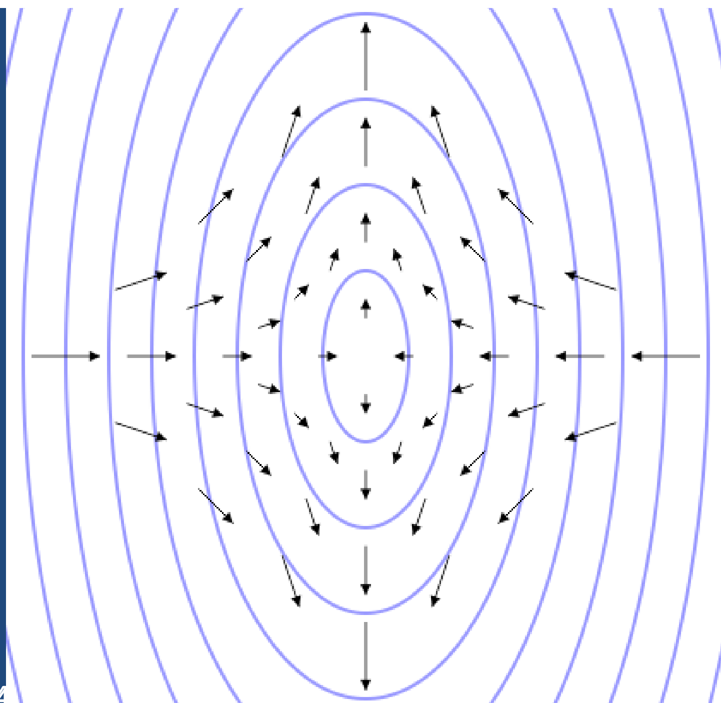

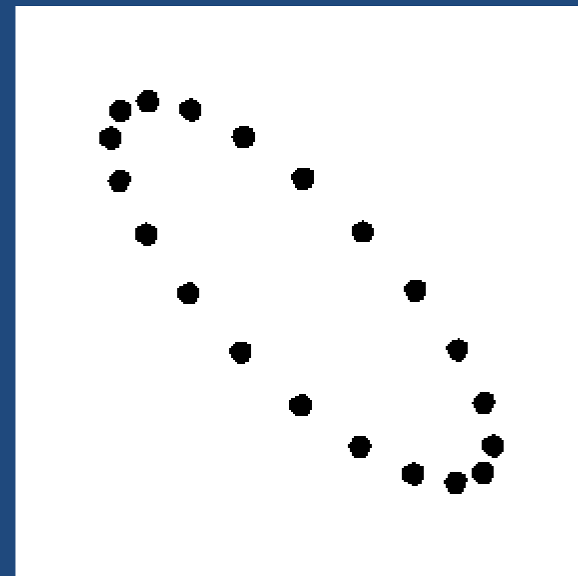

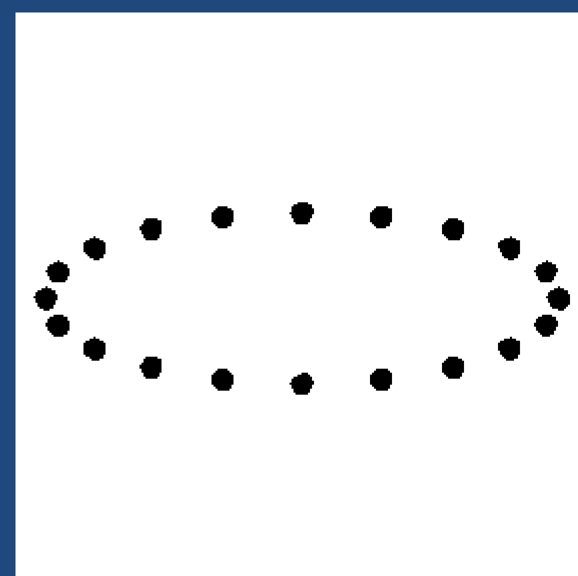

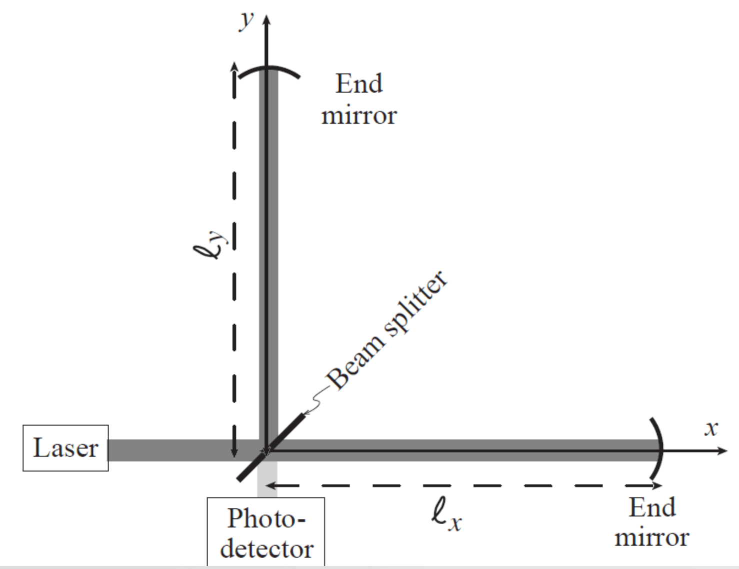

Laser interferometers

LIGO 1990-2017 ~690 MUSD

Chirp signal from coalescing binary system

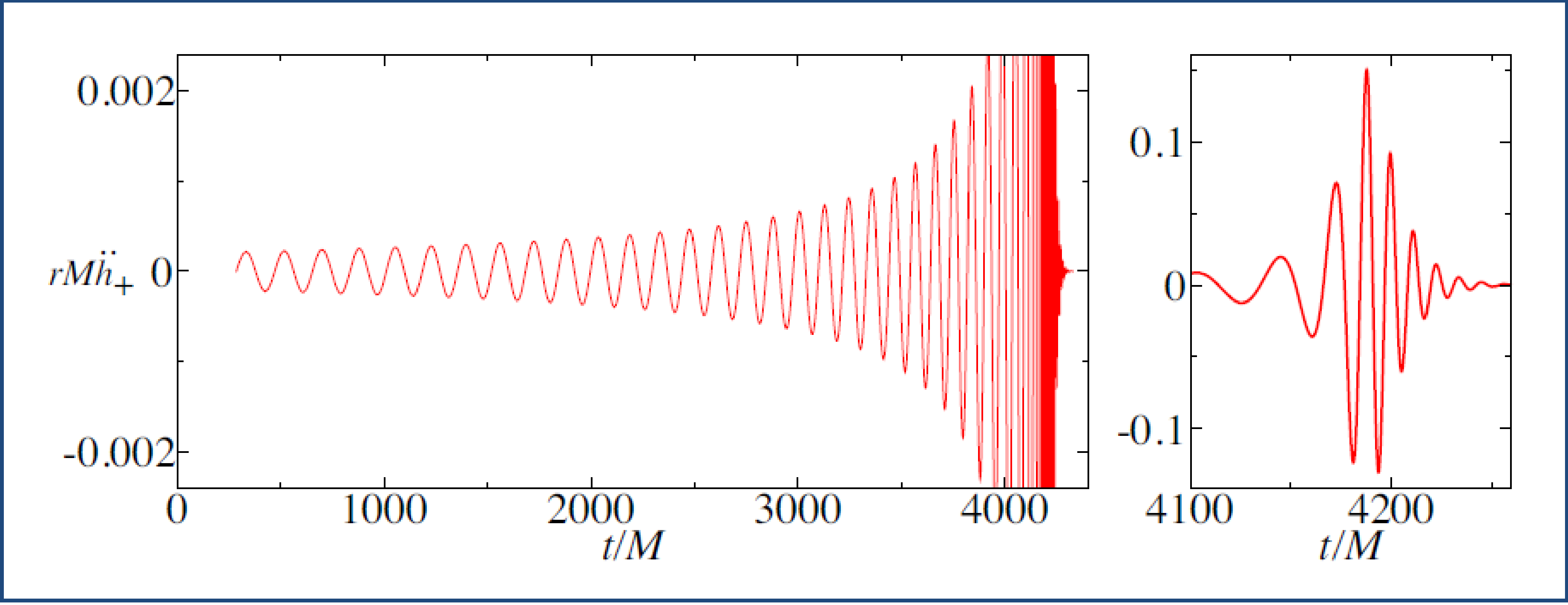

$$h_+ = h^{\rm TT}_{\hat\theta\hat\theta} = \frac{2}{r}[\ddot{I}_{\hat\theta\hat\theta}(t-r)]^{\rm TT} = -2(1+\cos^2\theta)\ \frac{\mu(M\Omega)^{2/3}}{r}\cos[2(\Omega t - \Omega r - \phi)]$$

$$h_\times = h^{\rm TT}_{\hat\theta\hat\phi} = \frac{2}{r}[\ddot{I}_{\hat\theta\hat\phi}(t-r)]^{\rm TT} = -4\cos\theta\ \frac{\mu(M\Omega)^{2/3}}{r}\sin[2(\Omega t - \Omega r - \phi)]\ .$$

GW from inspiraling binary BH

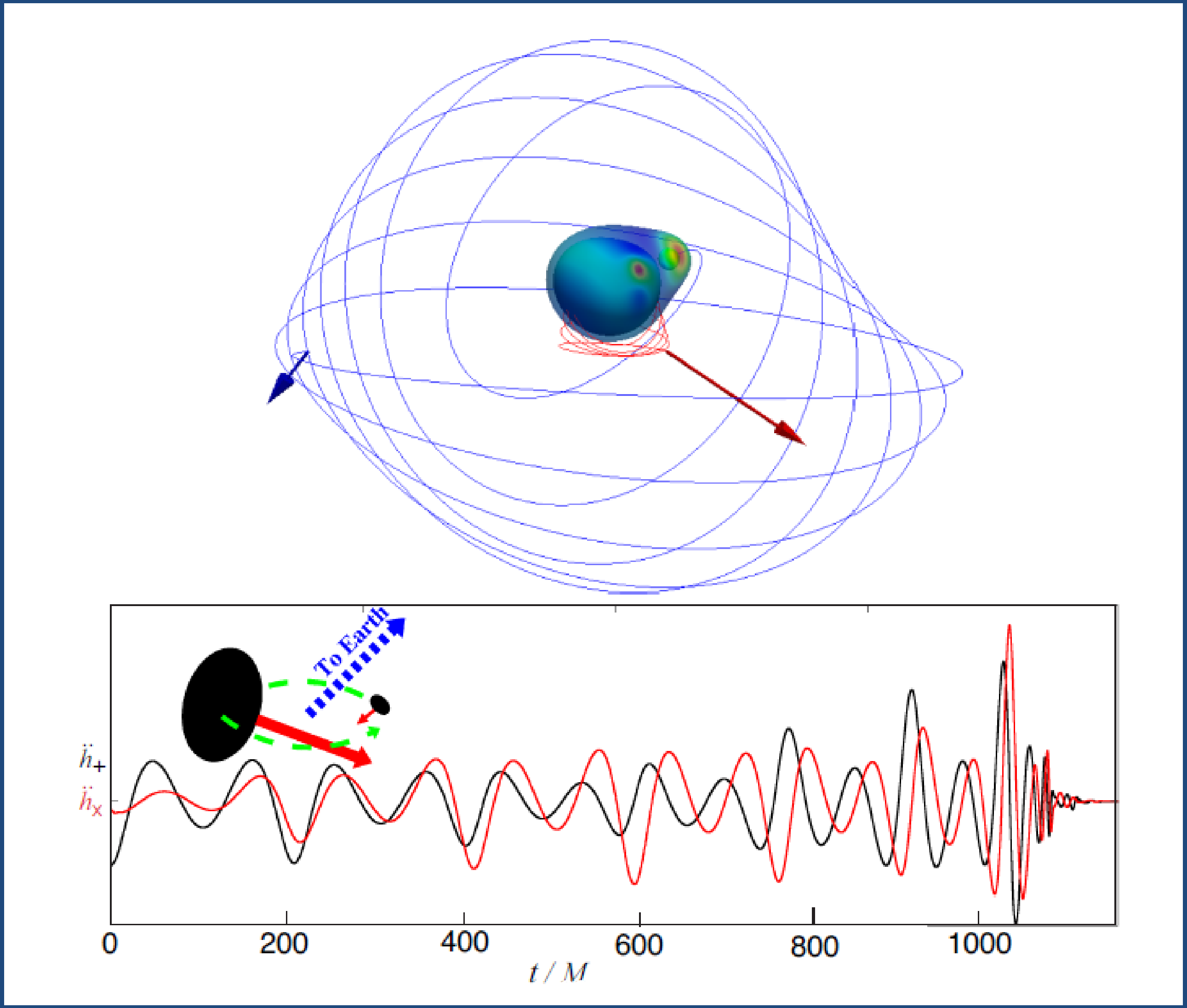

LIGO

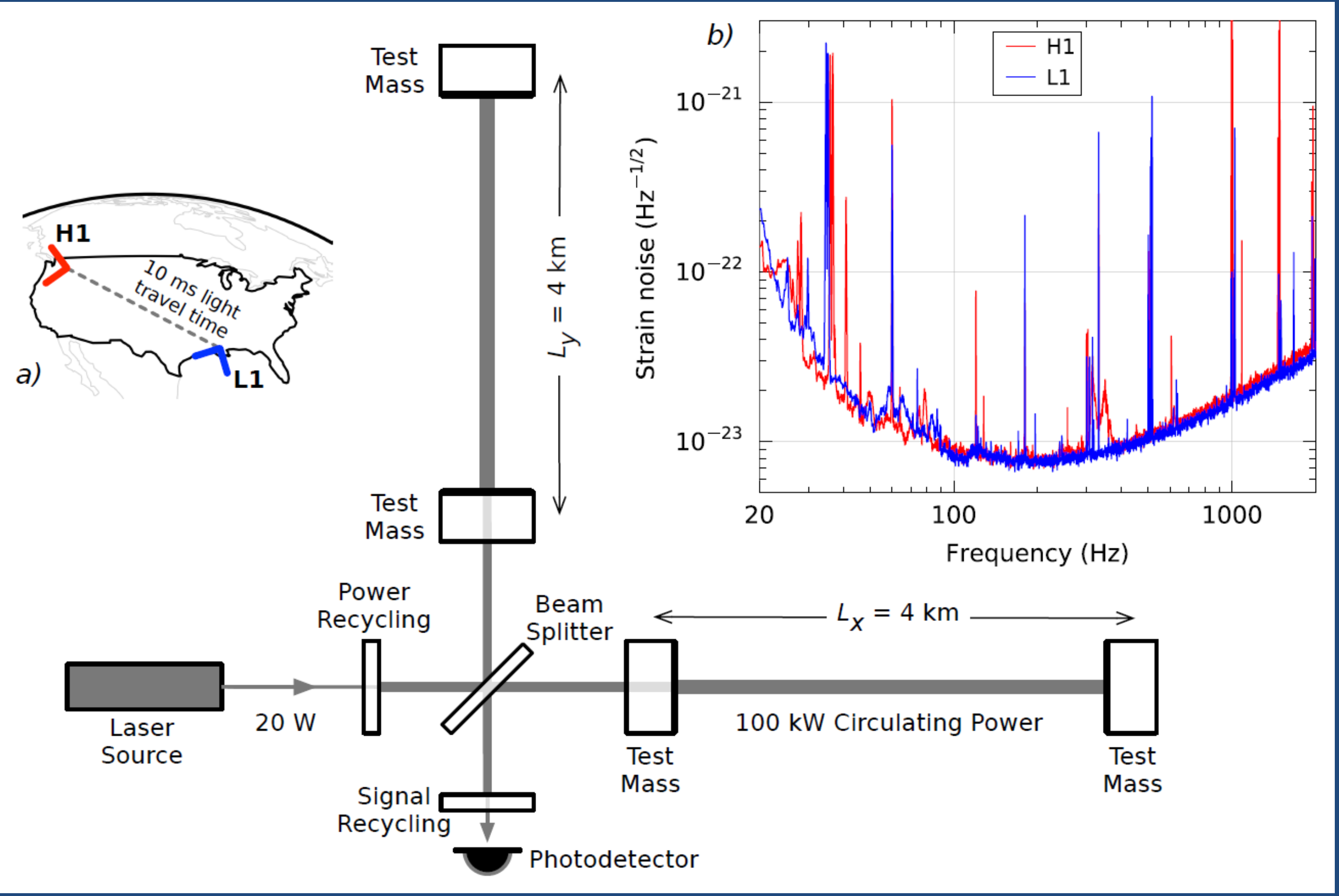

D. Reitze, 2017

Working GW-interferometers

LIGO
Hanford
USA

KAGRA
Kamioka
Japan

Virgo
Pisa
Italy

LIGO
Livingston
USA

Credit: LVC collab., Univ. of Tokyo

GW150914

PRL 116, 061102 (2016)

35-350 Hz bandpass filter applied

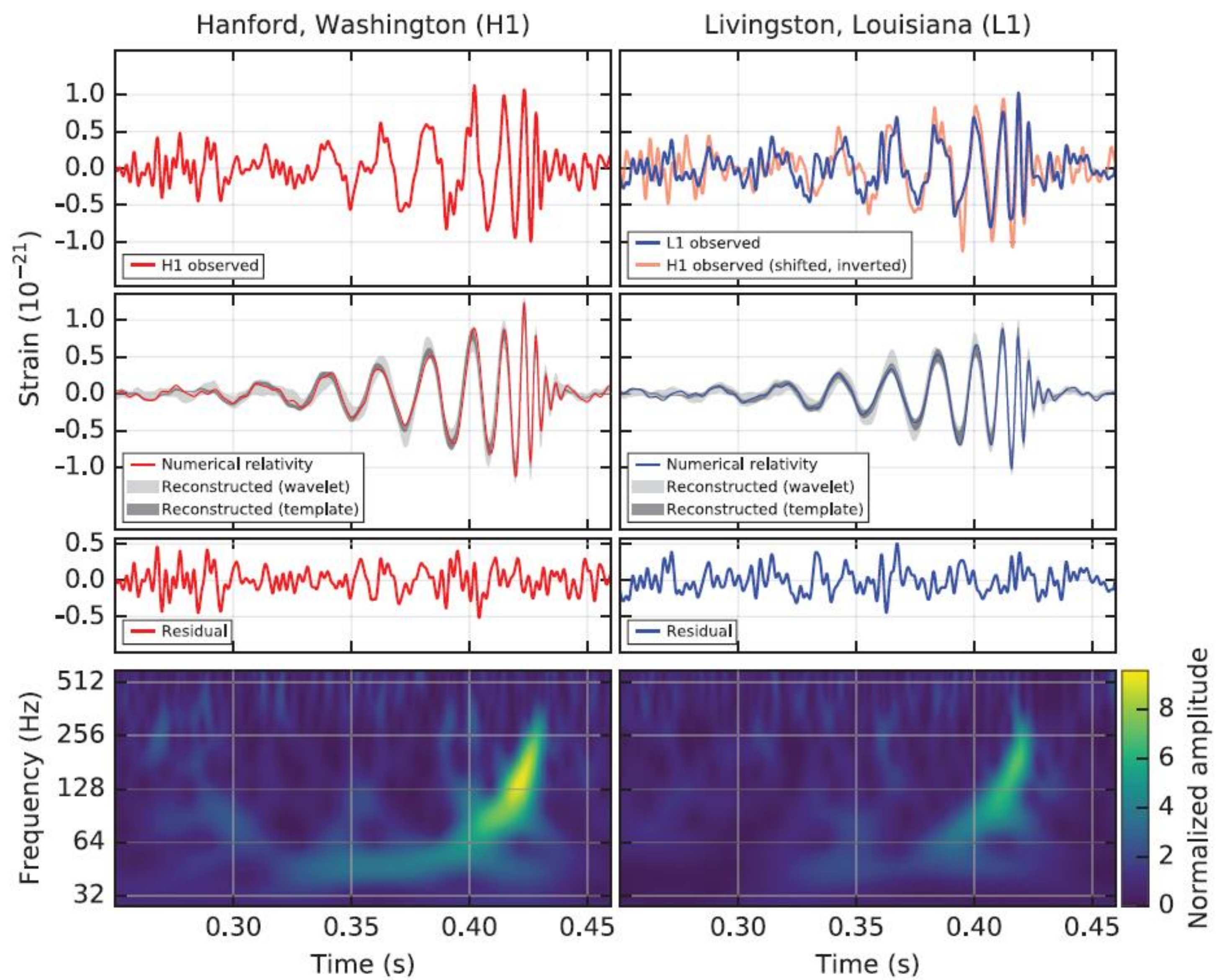

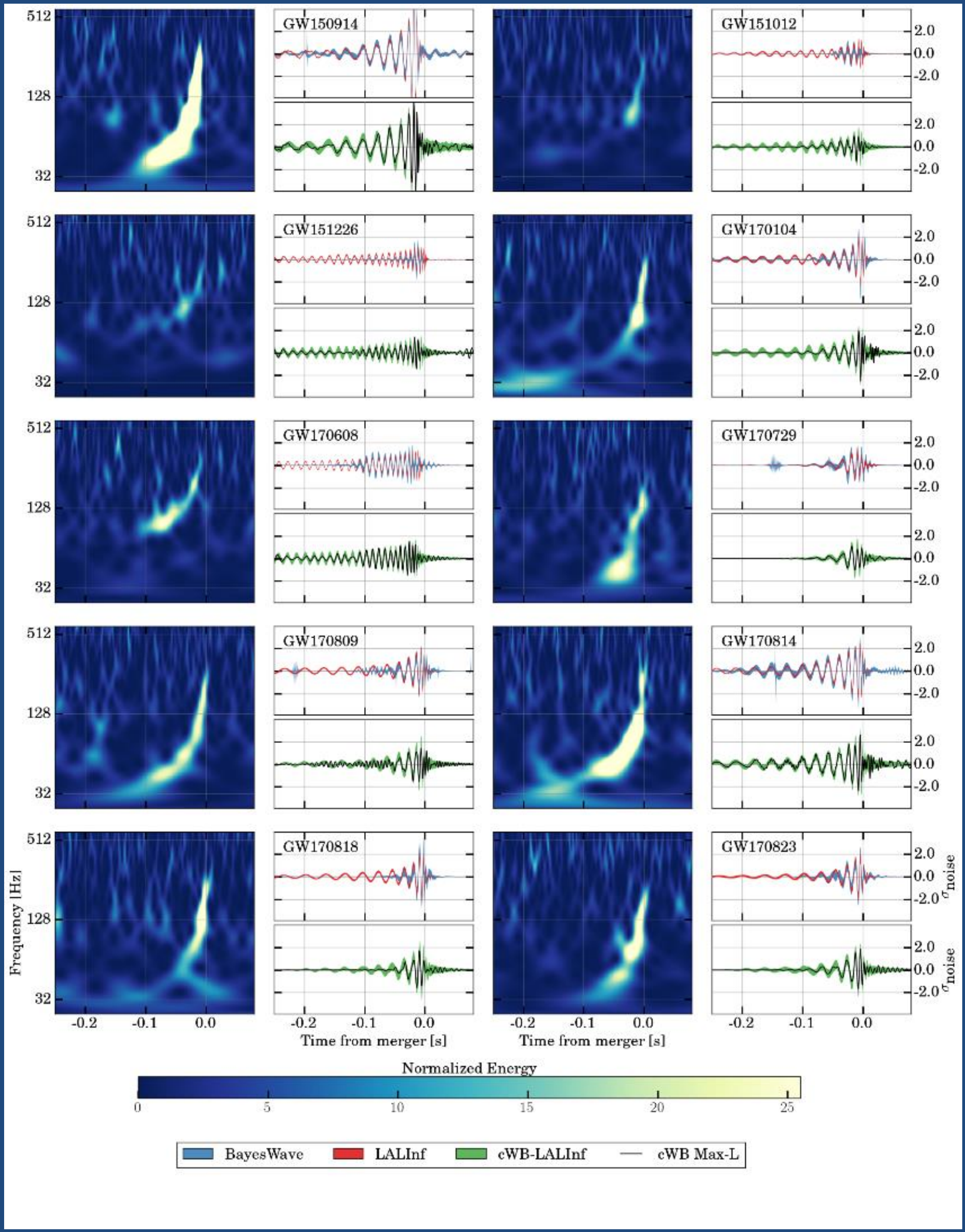

Binary BHs LIGO/Virgo

GWTC-1 Catalog arXiv:1811.12907

Chirp signal from inspiraling binaries

- Chirp-mass determined inspiraling signal

$$M_{ch} = (\mu^3 M^2)^{1/5}$$

$$h \sim M_{ch}^{5/3} f^{2/3} / r$$

$$\mathcal{M} = \frac{(m_1 m_2)^{3/5}}{(m_1 + m_2)^{1/5}} = \frac{c^3}{G}\left(\frac{5}{96}\pi^{-8/3} f^{-11/3} \dot{f}\right)^{3/5}$$

Chirp mass determines detection horizon. $h_{lim} \sim M^{(5/6)}$

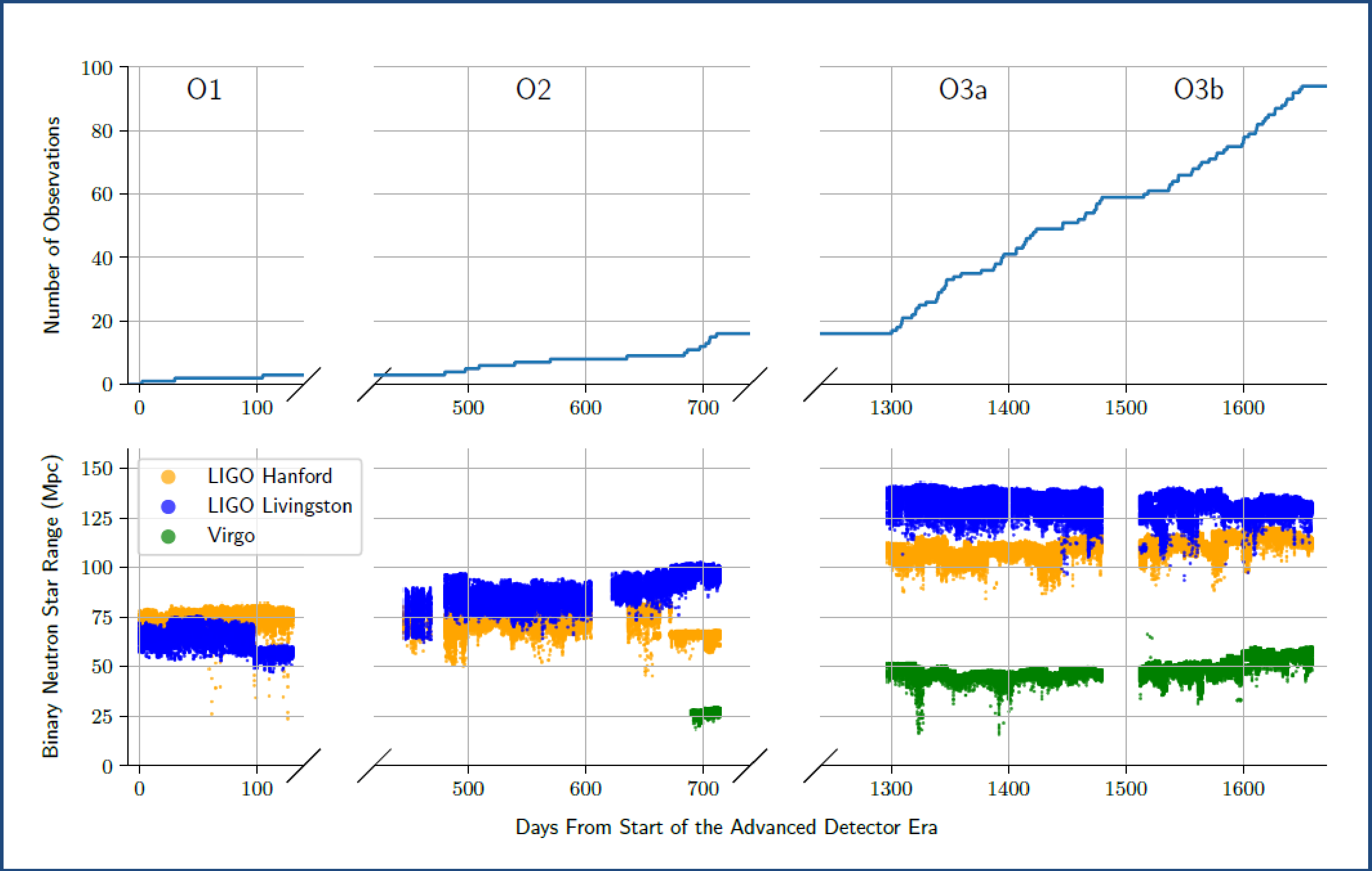

Mass-redshift degeneracy

$$f_0 = f/(1+z),\ \ dt_0 = dt(1+z)$$

$$\left.\frac{df}{dt}\right|_o = \frac{df}{dt}\frac{1}{(1+z)^2}$$

$$\left.M_{ch}\right|_o = \left(\frac{5 f_o^{-11/3}(df_o/dt)}{96\pi^{8/3}}\right)^{3/5} = M_{ch}(1+z) ==> \ fM_{ch} = inv$$

$$h_o \sim \frac{M_{ch}}{d_m}(\pi f M_{ch})^{2/3}$$

$$d_o \sim \frac{4(M_{ch})_o}{h_o}(\pi f_o (M_{ch})_o)^{2/3} = d_m(1+z)$$ Luminosity distance

1^{st} cosmological inference

- Coalescing binaries as cosmological “standard sirens” (B. Schutz, 1986)
- Photometric distance from GW signal + independent knowledge of redshift (e.g., from electromagnetic astronomy) ➔ test of cosmological models

Parameters from GW observations

$$\mathcal{M} = \frac{(m_1 m_2)^{3/5}}{M^{1/5}}$$

Chirp mass

$$\chi_{\rm eff} = \frac{(m_1\vec{\chi}_1 + m_2\vec{\chi}_2)\cdot\hat{L}_N}{M}$$

Effective spin

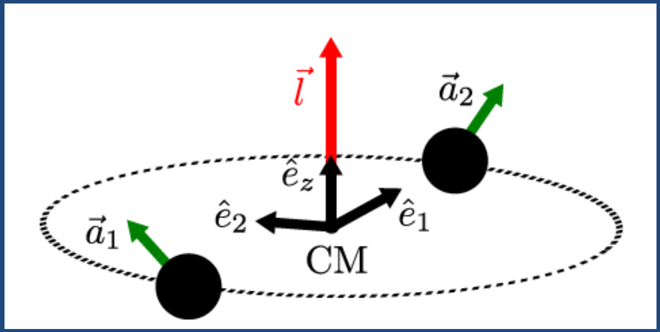

Event	$m_1/M_\odot$	$m_2/M_\odot$	$\mathcal{M}/M_\odot$	$\chi_{\rm eff}$	$M_f/M_\odot$	a_f	$E_{\rm rad}/(M_\odot c^2)$	$\ell_{\rm peak}/({\rm erg\,s^{-1}})$	d_L/Mpc	z	$\Delta\Omega/{\rm deg}^2$
GW150914	$35.6^{+4.8}_{-3.0}$	$30.6^{+3.0}_{-4.4}$	$28.6^{+1.6}_{-1.5}$	$-0.01^{+0.12}_{-0.13}$	$63.1^{+3.3}_{-3.0}$	$0.69^{+0.05}_{-0.04}$	$3.1^{+0.4}_{-0.4}$	$3.6^{+0.4}_{-0.4}\times10^{56}$	430^{+150}_{-170}	$0.09^{+0.03}_{-0.03}$	180
GW151012	$23.3^{+14.0}_{-5.5}$	$13.6^{+4.1}_{-4.8}$	$15.2^{+2.0}_{-1.1}$	$0.04^{+0.28}_{-0.19}$	$35.7^{+9.9}_{-3.8}$	$0.67^{+0.13}_{-0.11}$	$1.5^{+0.5}_{-0.5}$	$3.2^{+0.8}_{-1.7}\times10^{56}$	1060^{+540}_{-480}	$0.21^{+0.09}_{-0.09}$	1555
GW151226	$13.7^{+8.8}_{-3.2}$	$7.7^{+2.2}_{-2.6}$	$8.9^{+0.3}_{-0.3}$	$0.18^{+0.20}_{-0.12}$	$20.5^{+6.4}_{-1.5}$	$0.74^{+0.07}_{-0.05}$	$1.0^{+0.1}_{-0.2}$	$3.4^{+0.7}_{-1.7}\times10^{56}$	440^{+180}_{-190}	$0.09^{+0.04}_{-0.04}$	1033
GW170104	$31.0^{+7.2}_{-5.6}$	$20.1^{+4.9}_{-4.5}$	$21.5^{+2.1}_{-1.7}$	$-0.04^{+0.17}_{-0.20}$	$49.1^{+5.2}_{-3.9}$	$0.66^{+0.08}_{-0.10}$	$2.2^{+0.5}_{-0.5}$	$3.3^{+0.6}_{-0.9}\times10^{56}$	960^{+430}_{-410}	$0.19^{+0.07}_{-0.08}$	924
GW170608	$10.9^{+5.3}_{-1.7}$	$7.6^{+1.3}_{-2.1}$	$7.9^{+0.2}_{-0.2}$	$0.03^{+0.19}_{-0.07}$	$17.8^{+3.2}_{-0.7}$	$0.69^{+0.04}_{-0.04}$	$0.9^{+0.05}_{-0.1}$	$3.5^{+0.4}_{-1.3}\times10^{56}$	320^{+120}_{-110}	$0.07^{+0.02}_{-0.02}$	396
GW170729	$50.6^{+16.6}_{-10.2}$	$34.3^{+9.1}_{-10.1}$	$35.7^{+6.5}_{-4.7}$	$0.36^{+0.21}_{-0.25}$	$80.3^{+14.6}_{-10.2}$	$0.81^{+0.07}_{-0.13}$	$4.8^{+1.7}_{-1.7}$	$4.2^{+0.9}_{-1.5}\times10^{56}$	2750^{+1350}_{-1320}	$0.48^{+0.19}_{-0.20}$	1033
GW170809	$35.2^{+8.3}_{-6.0}$	$23.8^{+5.2}_{-5.1}$	$25.0^{+2.1}_{-1.6}$	$0.07^{+0.16}_{-0.16}$	$56.4^{+5.2}_{-3.7}$	$0.70^{+0.08}_{-0.09}$	$2.7^{+0.6}_{-0.6}$	$3.5^{+0.6}_{-0.9}\times10^{56}$	990^{+320}_{-380}	$0.20^{+0.05}_{-0.07}$	340
GW170814	$30.7^{+5.7}_{-3.0}$	$25.3^{+2.9}_{-4.1}$	$24.2^{+1.4}_{-1.1}$	$0.07^{+0.12}_{-0.11}$	$53.4^{+3.2}_{-2.4}$	$0.72^{+0.07}_{-0.05}$	$2.7^{+0.4}_{-0.3}$	$3.7^{+0.4}_{-0.5}\times10^{56}$	580^{+160}_{-210}	$0.12^{+0.03}_{-0.04}$	87
GW170817	$1.46^{+0.12}_{-0.10}$	$1.27^{+0.09}_{-0.09}$	$1.186^{+0.001}_{-0.001}$	$0.00^{+0.02}_{-0.01}$	≤ 2.8	≤ 0.89	≥ 0.04	$\geq 0.1\times10^{56}$	40^{+10}_{-10}	$0.01^{+0.00}_{-0.00}$	16
GW170818	$35.5^{+7.5}_{-4.7}$	$26.8^{+4.3}_{-5.2}$	$26.7^{+2.1}_{-1.7}$	$-0.09^{+0.18}_{-0.21}$	$59.8^{+4.8}_{-3.8}$	$0.67^{+0.07}_{-0.08}$	$2.7^{+0.5}_{-0.5}$	$3.4^{+0.5}_{-0.7}\times10^{56}$	1020^{+430}_{-360}	$0.20^{+0.07}_{-0.07}$	39
GW170823	$39.6^{+10.0}_{-6.6}$	$29.4^{+6.3}_{-7.1}$	$29.3^{+4.2}_{-3.2}$	$0.08^{+0.20}_{-0.22}$	$65.6^{+9.4}_{-6.6}$	$0.71^{+0.08}_{-0.10}$	$3.3^{+0.9}_{-0.8}$	$3.6^{+0.6}_{-0.9}\times10^{56}$	1850^{+840}_{-840}	$0.34^{+0.13}_{-0.14}$	1651

arXiv:1811.12907

Coalescing binaries LIGO/Virgo

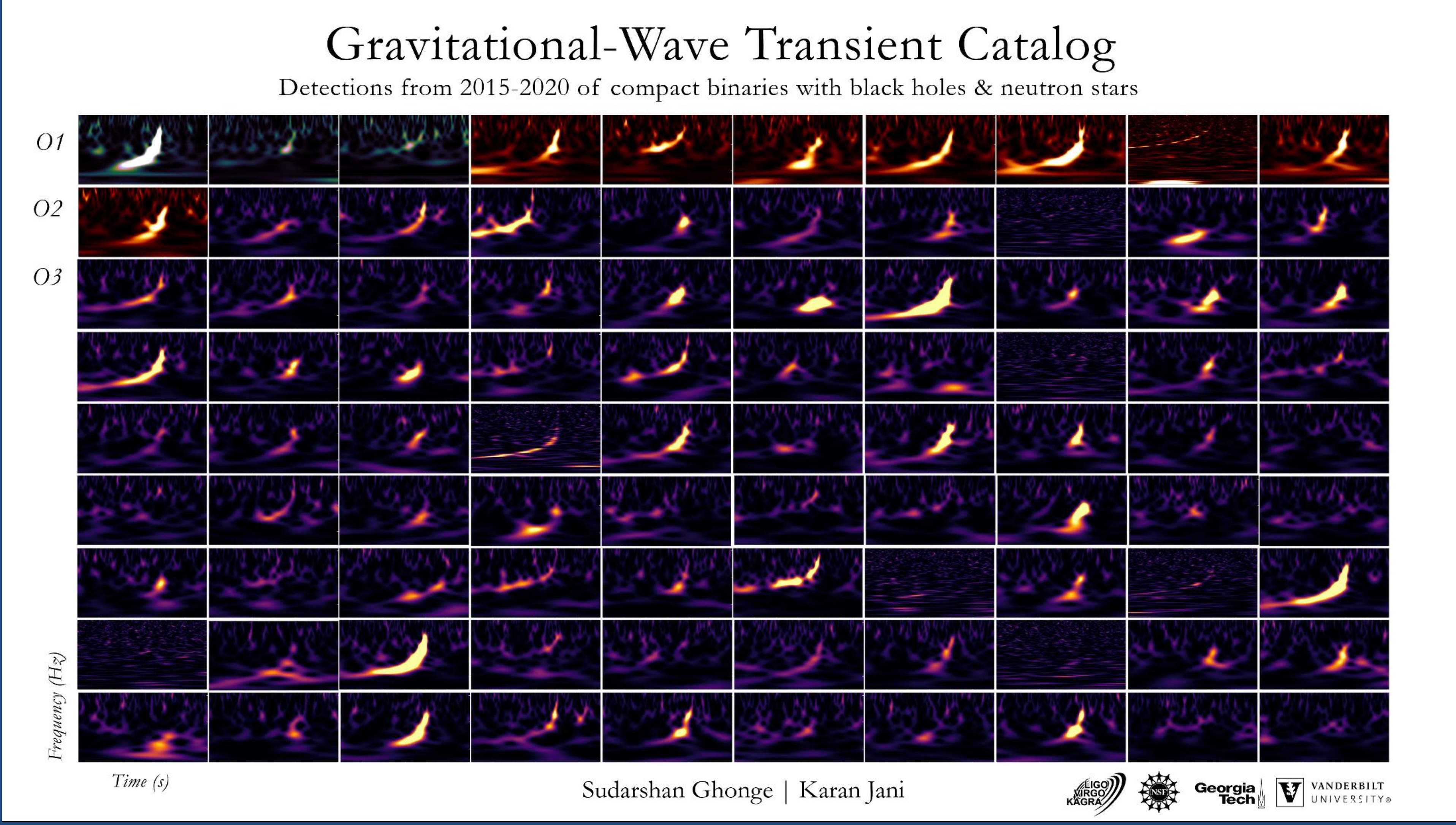

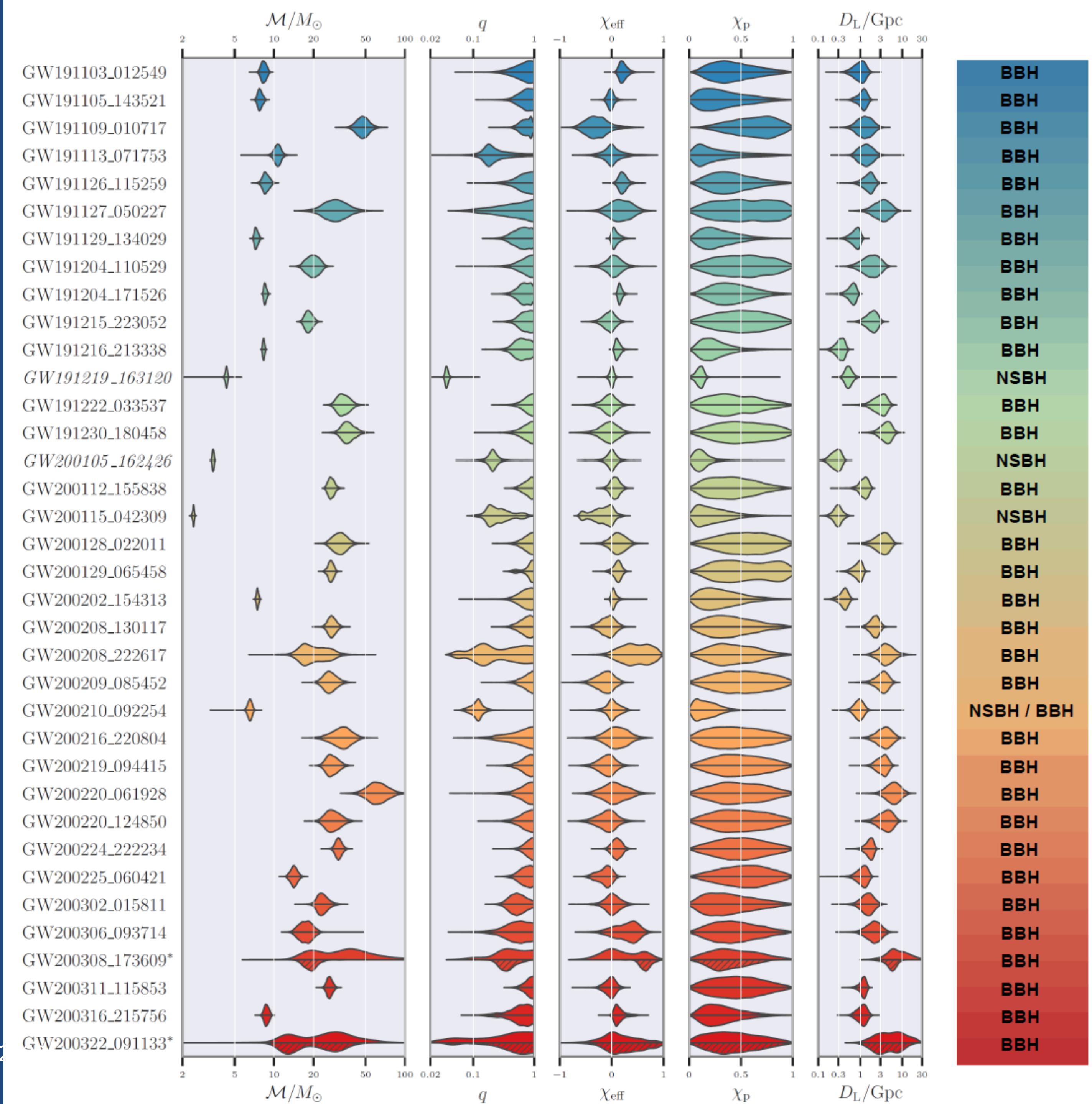

$\mathcal{M}/M_\odot$
q
$\chi_{\rm eff}$
$\chi_{\rm p}$
$D_{\rm L}/{\rm Gpc}$
2 5 10 20 50 100
0.02 0.1 1
−1 0 1
0 0.5 1
0.1 0.3 1 3 10 30
GW191103_012549 BBH
GW191105_143521 BBH
GW191109_010717 BBH
GW191113_071753 BBH
GW191126_115259 BBH
GW191127_050227 BBH
GW191129_134029 BBH
GW191204_110529 BBH
GW191204_171526 BBH
GW191215_223052 BBH
GW191216_213338 BBH
GW191219_163120 NSBH
GW191222_033537 BBH
GW191230_180458 BBH
GW200105_162426 NSBH
GW200112_155838 BBH
GW200115_042309 NSBH
GW200128_022011 BBH
GW200129_065458 BBH
GW200202_154313 BBH
GW200208_130117 BBH
GW200208_222617 BBH
GW200209_085452 BBH
GW200210_092254 NSBH / BBH
GW200216_220804 BBH
GW200219_094415 BBH
GW200220_061928 BBH
GW200220_124850 BBH
GW200224_222234 BBH
GW200225_060421 BBH
GW200302_015811 BBH
GW200306_093714 BBH
GW200308_173609* BBH
GW200311_115853 BBH
GW200316_215756 BBH
GW200322_091133* BBH

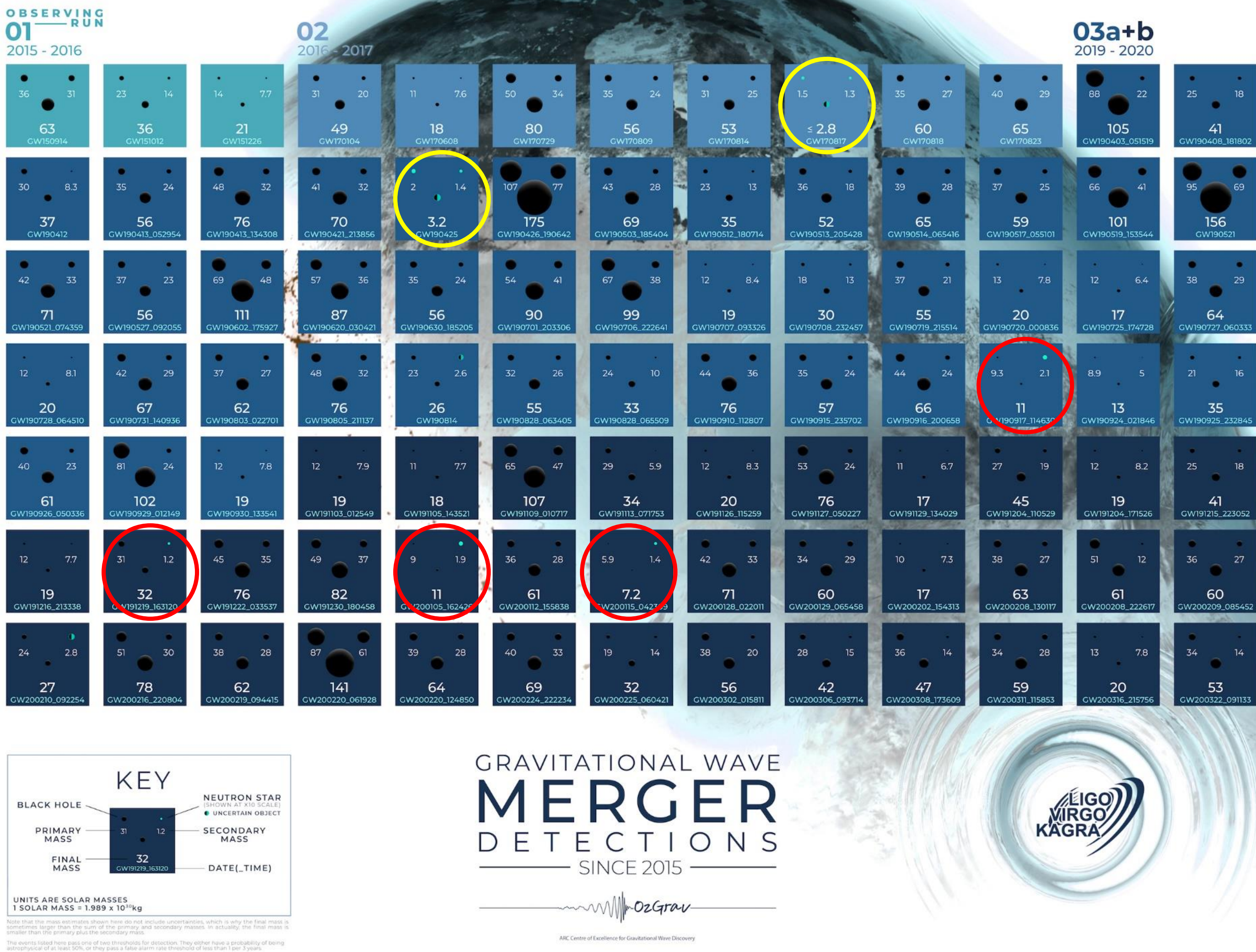
OBSERVING RUN
01 2015 - 2016
02 2016 - 2017
03a+b 2019 - 2020
36 31 63 GW150914
23 14 36 GW151012
14 7.7 21 GW151226
31 20 49 GW170104
11 7.6 18 GW170608
50 34 80 GW170729
35 24 56 GW170809
31 25 53 GW170814
1.5 1.3 ≤ 2.8 GW170817
35 27 60 GW170818
40 29 65 GW170823
88 22 105 GW190403_051519
25 18 41 GW190408_181802
30 8.3 37 GW190412
35 24 56 GW190413_052954
48 32 76 GW190413_134308
41 32 70 GW190421_213856
2 1.4 3.2 GW190425
107 77 175 GW190426_190642
43 28 69 GW190503_185404
23 13 35 GW190512_180714
36 18 52 GW190513_205428
39 28 65 GW190514_065416
37 25 59 GW190517_055101
66 41 101 GW190519_153544
95 69 156 GW190521
42 33 71 GW190521_074359
37 23 56 GW190527_092055
69 48 111 GW190602_175927
57 36 87 GW190620_030421
35 24 56 GW190630_185205
54 41 90 GW190701_203306
67 38 99 GW190706_222641
12 8.4 19 GW190707_093326
18 13 30 GW190708_232457
37 21 55 GW190719_215514
13 7.8 20 GW190720_000836
12 6.4 17 GW190725_174728
38 29 64 GW190727_060333
12 8.1 20 GW190728_064510
42 29 67 GW190731_140936
37 27 62 GW190803_022701
48 32 76 GW190805_211137
23 2.6 26 GW190814
32 26 55 GW190828_063405
24 10 33 GW190828_065509
44 36 76 GW190910_112807
35 24 57 GW190915_235702
44 24 66 GW190916_200658
9.3 2.1 11 GW190917_114630
8.9 5 13 GW190924_021846
21 16 35 GW190925_232845
40 23 61 GW190926_050336
81 24 102 GW190929_012149
12 7.8 19 GW190930_133541
12 7.9 19 GW191103_012549
11 7.7 18 GW191105_143521
65 47 107 GW191109_010717
29 5.9 34 GW191113_071753
12 8.3 20 GW191126_115259
53 24 76 GW191127_050227
11 6.7 17 GW191129_134029
27 19 45 GW191204_110529
12 8.2 19 GW191204_171526
25 18 41 GW191215_223052
12 7.7 19 GW191216_213338
31 1.2 32 GW191219_163120
45 35 76 GW191222_033537
49 37 82 GW191230_180458
9 1.9 11 GW200105_162426
36 28 61 GW200112_155838
5.9 1.4 7.2 GW200115_042309
42 33 71 GW200128_022011
34 29 60 GW200129_065458
10 7.3 17 GW200202_154313
38 27 63 GW200208_130117
51 12 61 GW200208_222617
36 27 60 GW200209_085452
24 2.8 27 GW200210_092254
51 30 78 GW200216_220804
38 28 62 GW200219_094415
87 61 141 GW200220_061928
39 28 64 GW200220_124850
40 33 69 GW200224_222234
19 14 32 GW200225_060421
38 20 56 GW200302_015811
28 15 42 GW200306_093714
36 14 47 GW200308_173609
34 28 59 GW200311_115853
13 7.8 20 GW200316_215756
34 14 53 GW200322_091133
KEY
BLACK HOLE
NEUTRON STAR (SHOWN AT X10 SCALE)
UNCERTAIN OBJECT
PRIMARY MASS
SECONDARY MASS
FINAL MASS
DATE(_TIME)
31 1.2 32 GW191219_163120
UNITS ARE SOLAR MASSES
1 SOLAR MASS = 1.989 x 10³⁰kg
GRAVITATIONAL WAVE
MERGER
DETECTIONS
SINCE 2015
OzGrav
ARC Centre of Excellence for Gravitational Wave Discovery
LIGO
VIRGO
KAGRA

Statistical properties: summary

- O1+O2+O3: 91 robust (S/N>8) detections
- Isotropic on the sky (2207.05792)
- Signal properties in agreement with GR up to a few % accuracy
- 2 NS+NS mergings, EM from GW 170817
- 4 BH+NS candidates. No electromagnetic signals.

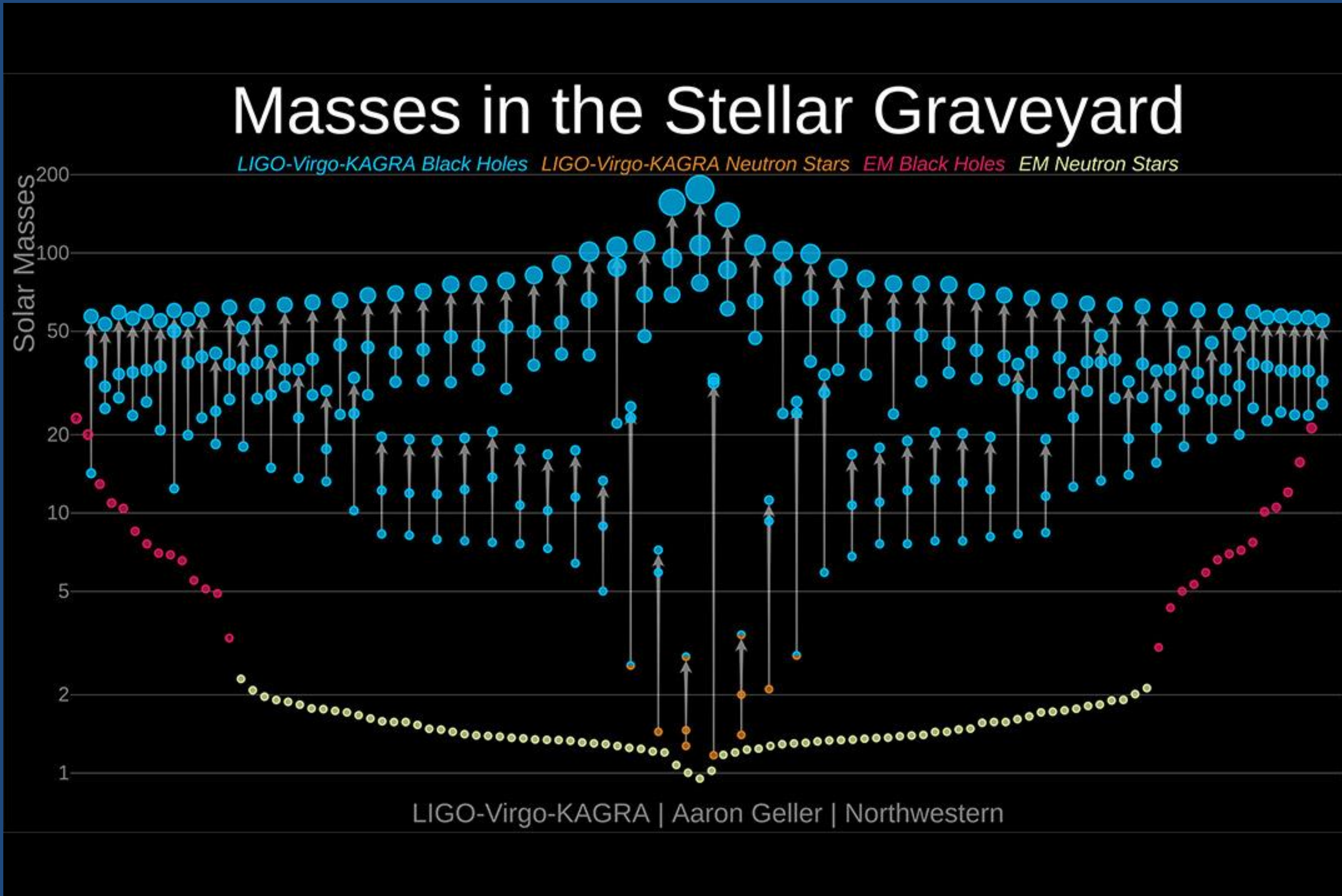

Masses in the Stellar Graveyard
LIGO-Virgo-KAGRA Black Holes
LIGO-Virgo-KAGRA Neutron Stars
EM Black Holes
EM Neutron Stars
Solar Masses
200
100
50
20
10
5
2
1
LIGO-Virgo-KAGRA | Aaron Geller | Northwestern

Exceptional BHBH mergers

- GW 190814, M_1=26 , q=0.112, M_2=2.6 in lower mass gap? NS? Strange quark star? Outlier population? Formation from a triple star? Formation in AGN disk? Primordial BH?
- GW190521 $m_1 = 85^{+21}_{-14}\,\mathrm{M}_\odot$ $m_2 = 66^{+17}_{-18}\,\mathrm{M}_\odot$n upper mass gap (60-120), large effective spin $\chi_{1,2}\sim 0.1$–$0.9)$

(Or even $m_1 = 168^{+15}_{-61}\,\mathrm{M}_\odot$ $m_2 = 66^{+33}_{-3}\,\mathrm{M}_\odot$??)

Repeated meggers in stellar clusters or AGN disks?? Primordial BH?

- GW190412 $m_1 = 30.1^{+4.6}_{-5.3}\,\mathrm{M}_\odot$ $m_2 = 8.3^{+1.6}_{-0.9}\,\mathrm{M}_\odot$ high spin $\chi_1 = 0.44^{+0.16}_{-0.22}$

→ Hierarchical merger?

Simplest scenario:
BH+BH from massive star evolution

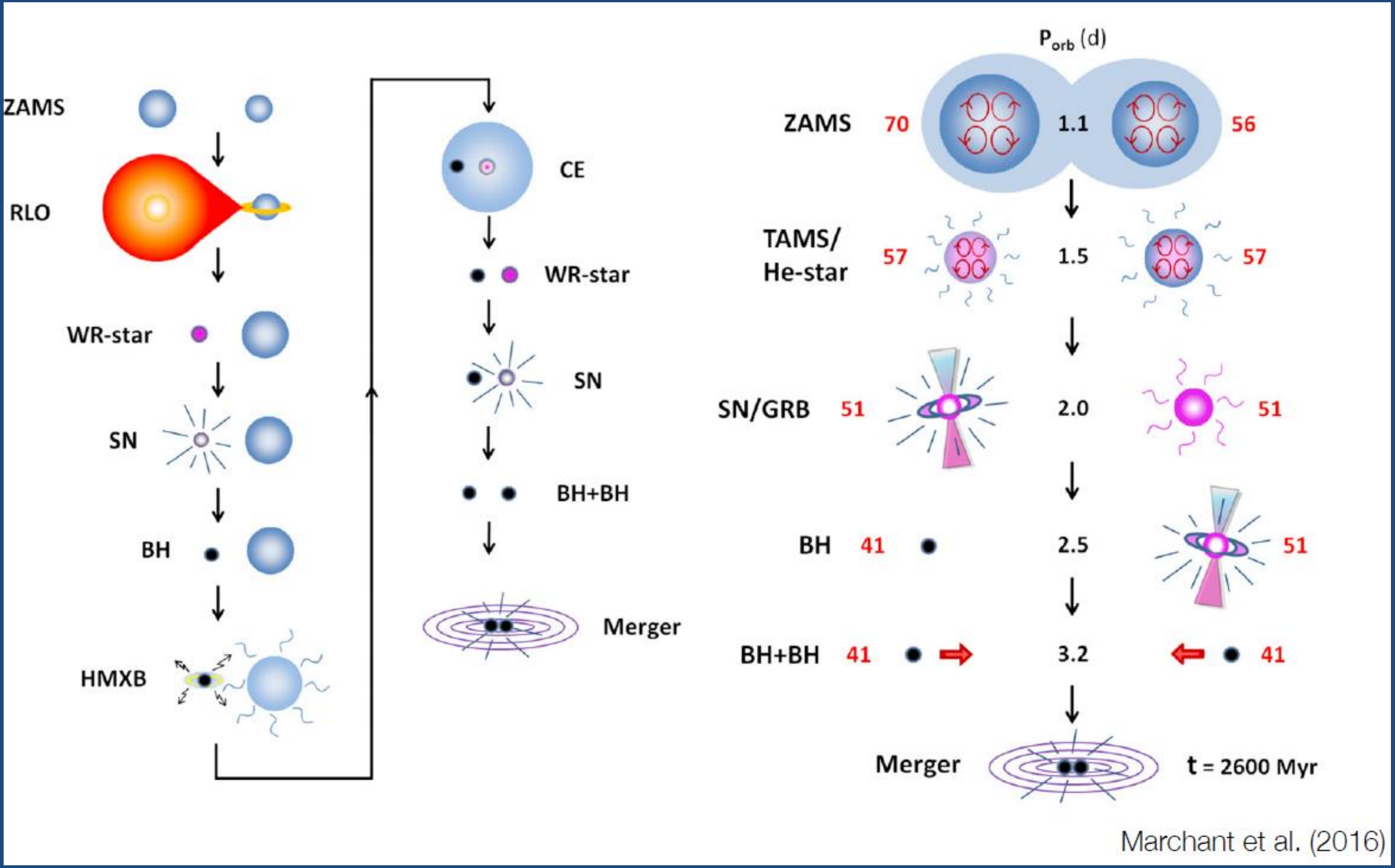

Astrophysical issues:
BH from stellar collapses, binary BH formation

- Mass loss from massive stars
- BH mass gaps (2.5-5, 60-130 M_{sun})
- BH kicks
- BH spins
- …

Other scenarios

Dynamical capture in dens stellar clusters (can produce BH with M>50 and non-parallel BH spins)

- "Exotic" scenarios – primordial BH (Zeldovich,Novikov 1967…Carr 1975… Dolgov&Silk 1993…)

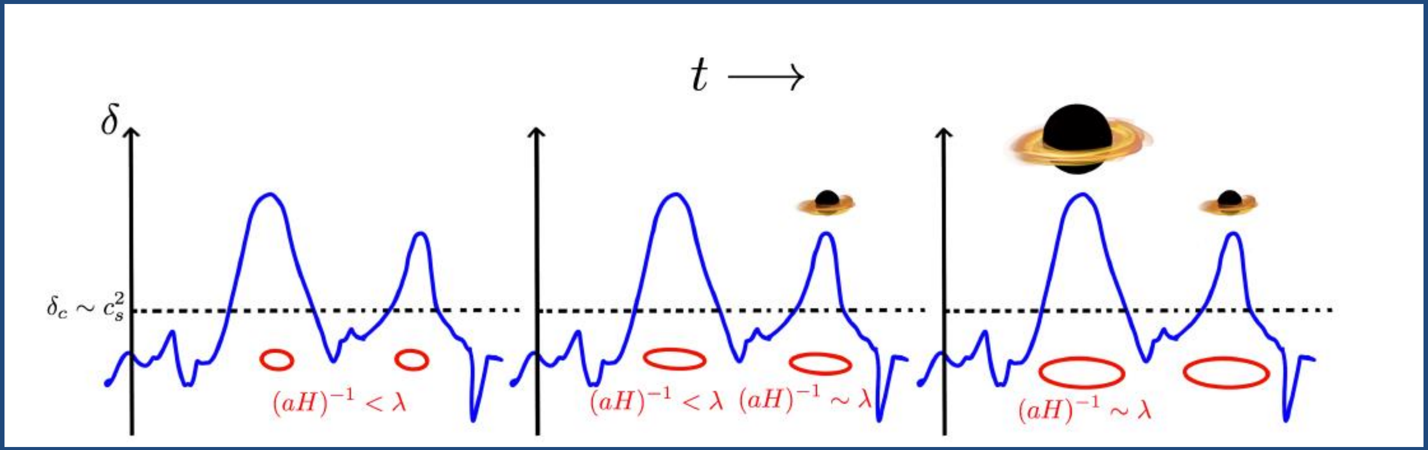

GW190521 as hyperbolic encounter of non-spinning BHs?

Table 1 | Source parameters of GW190521 with median values and 90% credible intervals quoted and natural logarithms reported

Reference[a]	This paper					LVK[4]	Gayathri et al.[15]	Romero-Shaw et al.[16]
Waveform	TEOBResumS[30,31]	TEOBResumS[30,31]	TEOBResumSP[44b]	NRSur7dq4 (ref.[42])	NRSur7dq4 (ref.[42])	NRSur7dq4 (ref.[42])	NR[47]	SEOBNRE[52]
E_0 prior	Unconstrained (UE_0)	Constrained (CE_0)	–	–	–	–	–	
Multipoles	$(\ell,\lvert m\rvert)=(2,2)$	$(\ell,\lvert m\rvert)=(2,2)$	$(\ell,\lvert m\rvert)=(2,2)$	$(\ell,\lvert m\rvert)=(2,2)$	$\ell\leq4$	$\ell\leq4$	–	–
$m_1\,(M_\odot)$	85^{+88}_{-22}	81^{+62}_{-25}	90^{+19}_{-14}	102^{+35}_{-23}	84^{+17}_{-12}	85^{+21}_{-14}	102^{+7}_{-11}	92^{+26}_{-16}
$m_2\,(M_\odot)$	59^{+18}_{-37}	52^{+32}_{-32}	66^{+10}_{-8}	64^{+19}_{-25}	71^{+16}_{-18}	66^{+17}_{-18}	102^{+7}_{-11}	69^{+18}_{-19}
$M_{source}\,(M_\odot)$[c]	151^{+73}_{-51}	130^{+75}_{-43}	156^{+25}_{-15}	164^{+40}_{-23}	153^{+29}_{-19}	150^{+29}_{-17}	–	–
$m_2/m_1\leq1$	$0.69^{+0.27}_{-0.52}$	$0.63^{+0.31}_{-0.43}$	$0.73^{+0.21}_{-0.15}$	$0.62^{+0.32}_{-0.30}$	$0.86^{+0.12}_{-0.30}$	$0.79^{+0.19}_{-0.29}$	–	–
χ_{eff}[d]	–	–	$-0.05^{+0.09}_{-0.12}$	$0.01^{+0.24}_{-0.26}$	$-0.03^{+0.25}_{-0.26}$	$0.08^{+0.27}_{-0.36}$	0	$0.0^{+0.2}_{-0.2}$
χ_p[e]	–	–	$0.72^{+0.16}_{-0.22}$	$0.71^{+0.22}_{-0.36}$	$0.79^{+0.16}_{-0.40}$	$0.68^{+0.25}_{-0.37}$	0.7	–
Eccentricity	–	–	–	–	–	–	0.67	0.11[f]
E_0/M	$1.014^{+0.009}_{-0.012}$	$1.014^{+0.010}_{-0.012}$	–	–	–	–	–	–
p^0_φ	$4.18^{+0.50}_{-0.62}$	$4.24^{+0.57}_{-0.37}$	–	–	–	–	–	–
Luminosity distance D_L (Gpc)	$4.7^{+4.8}_{-2.7}$	$6.1^{+3.3}_{-3.7}$	$4.5^{+1.2}_{-1.2}$	$3.9^{+2.3}_{-1.9}$	$4.8^{+2.3}_{-2.2}$	$5.3^{+2.4}_{-2.6}$	$1.84^{+1.07}_{-0.054}$	$4.1^{+1.8}_{-1.8}$
SNR_{max}	15.2	15.4	14.7	14.7	14.6	15.4	–	–
$\log(L)_{max}$	123.2	123.0	106.0	107.0	105.6	–	–	–
$\log B^{signal}_{noise}$	84.00±0.18	83.30±0.18	72.95±0.08	74.76±0.11	74.86±0.11	–	–	–

[a]Results of other analyses[4,15,16] are included for reference [b]Spin results obtained at a reference frequency of 5 Hz [c]Total mass in the frame of the source [d]Effective spin along the orbital angular momentum [e]Effective precessing spin[4] [f]Lower limit at 10 Hz

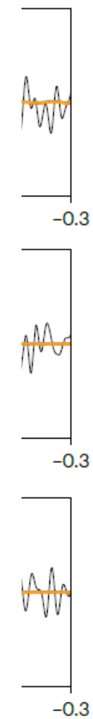

Gamba+'22, Nat. Ast.

Primordial Black Holes: formation

Zeldovich, Novikov’67, Carr, Hawking’74….

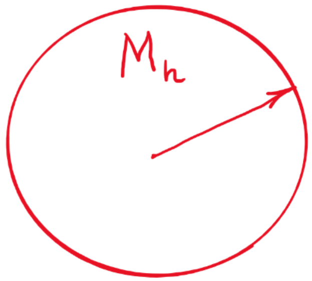

$$r_h = 2t \qquad M_h = m_{pl}^2\, t$$

$$\simeq 2.2\times 10^5 M_\odot \frac{t}{1s} \simeq 8 M_\odot \left(\frac{100\,\mathrm{MeV}}{T_{QCD}}\right)^2 \left(\frac{40}{g_*}\right)^{1/2}$$

$$\boxed{\frac{\delta\rho}{\rho} \gtrsim \left(\frac{M_h}{M}\right)^2}$$

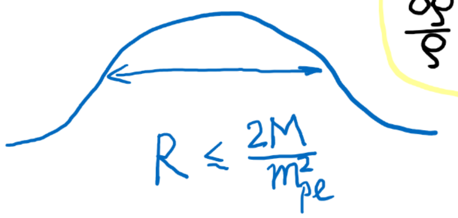

Dolgov+KP 2004.1699

Some PBH formation scenarios

- Primordial density fluctuations, $\delta>\delta_c\sim0.45$ (model-dependent)
- Collapse of scale-invariant fluctuations ➔ power-law mass spectra $dn/dM\sim M^{-\alpha}$, $\alpha=2(1+2w)/(1+w) = 2.5$ at RD ($w=1/3$)
- Inflationary models ➔ log-normal mass spectrum

$$\frac{dn}{dM} = \mu^2 \exp\left[-\gamma \ln^2(M/M_{max})\right]$$

(AD+Silk 1993)

- QCD phase transition at T=100-200 MeV:

$$M \sim \left(\frac{m_{Pl}}{m_p}\right)^3 m_p \sim M_{Ch} \sim 1 M_\odot$$

- Bubble collisions, cosmic strings …

Example: log-normal PBH mass function GWTC1+GWTC2

$$F(M) = A \exp[-\gamma \ln^2(M/M_0)]$$

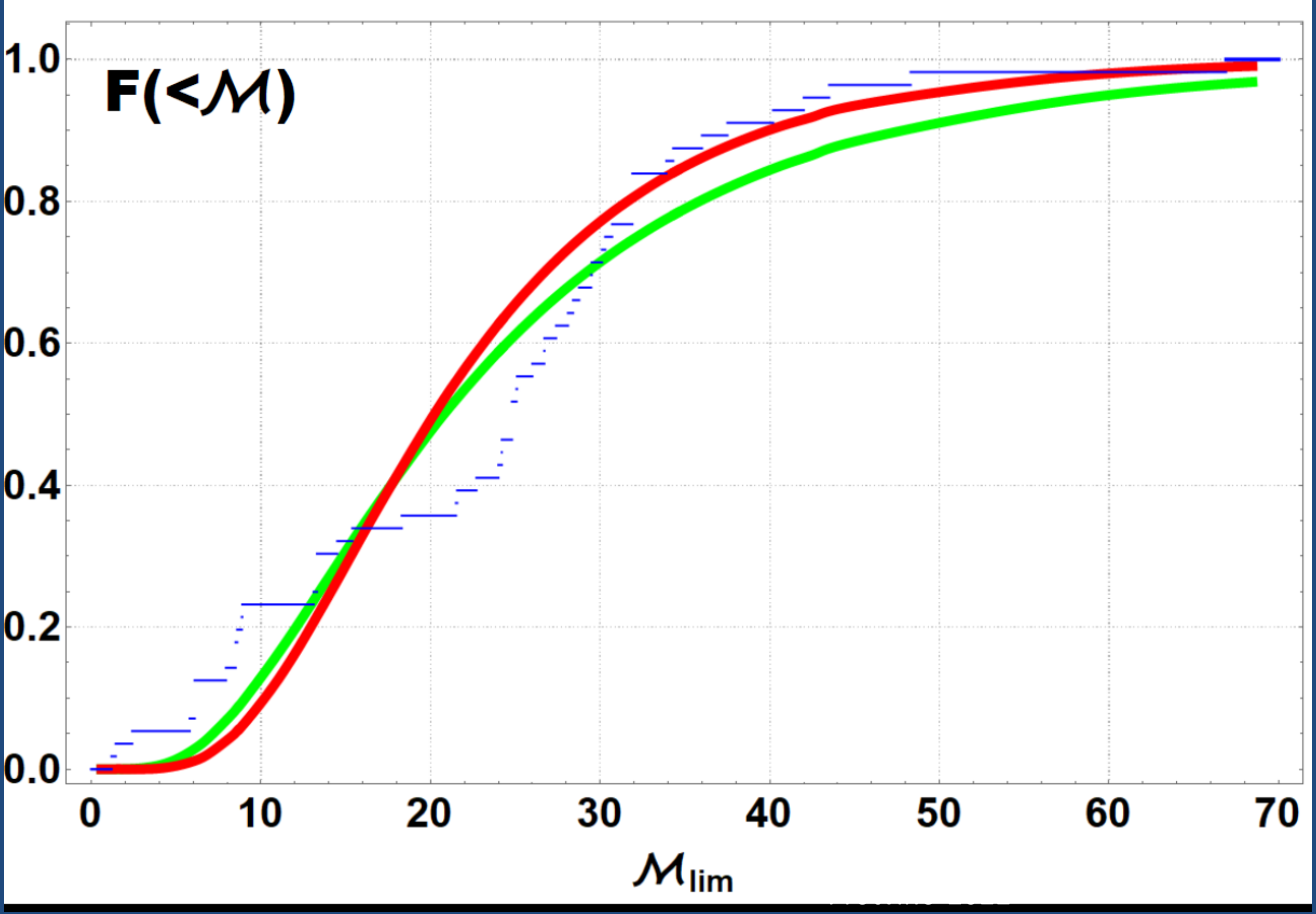

$$\gamma = 0.7,\ M_0 = 19$$

$$\mathrm{DR}(M_{ch})dM_{ch} \sim Ae^{-B\ln^2\left(\frac{M_{ch}}{M_0}\right)}dM_{ch}$$

Dolgov+'19

Astrophysical BHs +PBHs vs GWTC-3

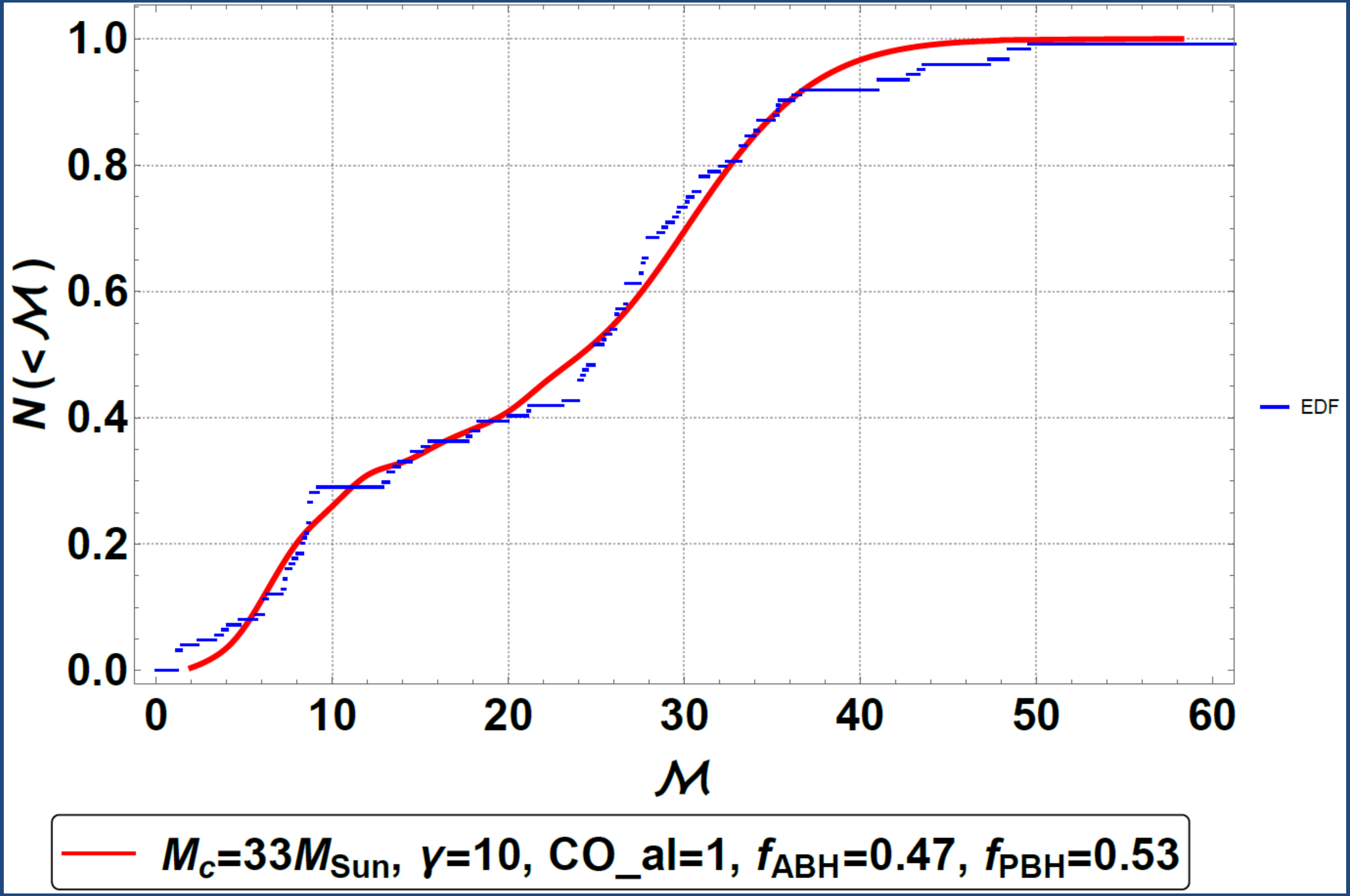

Effective spin – mass ratio correlation

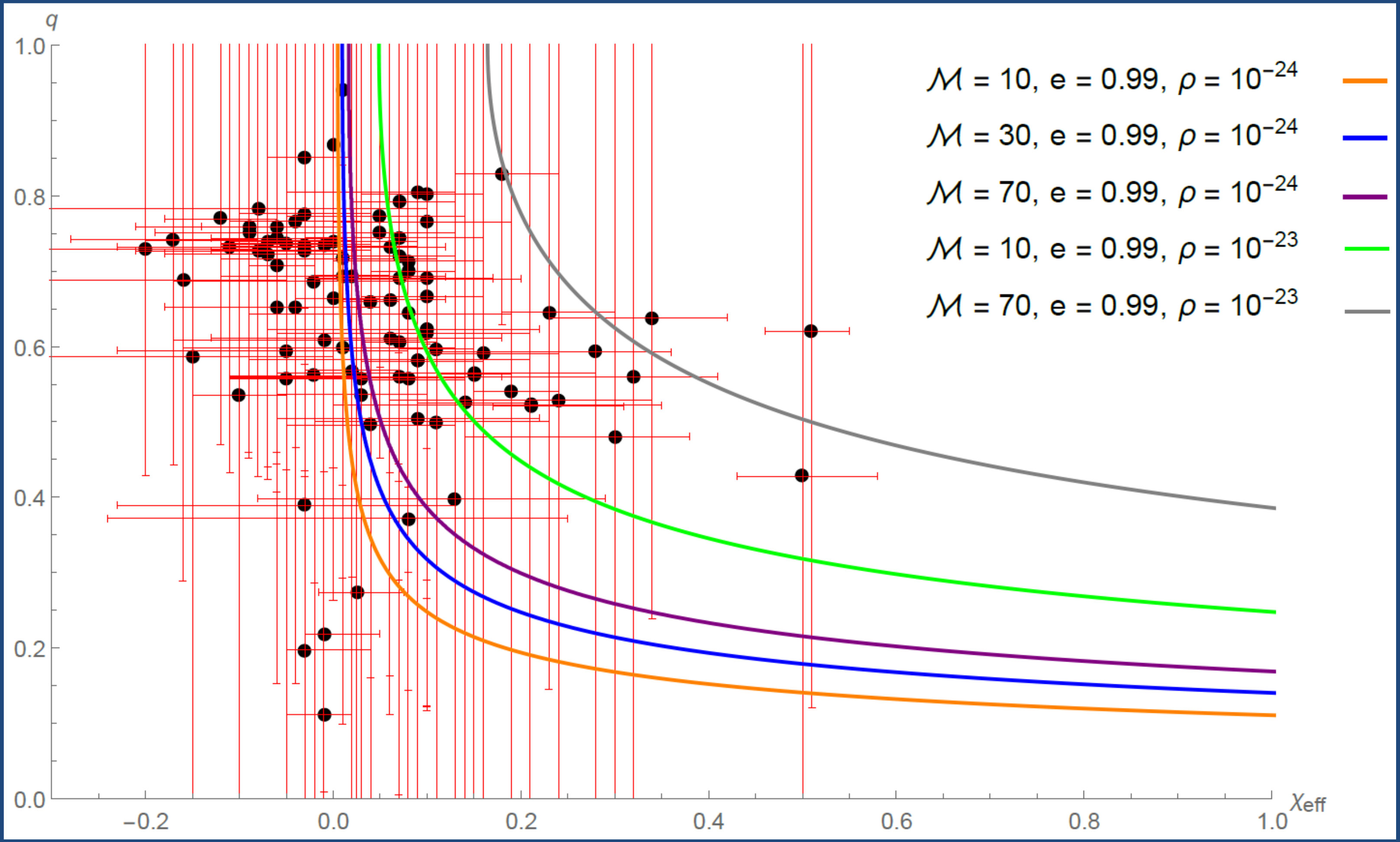

PK, Mitichkin 2211.03142

2d cosmological inference:

- Possibility of primordial binary BHs as (some) LVK GW sources (chirp-masses, effective spin – mass ratio correlation)
- → PBH with masses up $10^4\ M_\odot$ as seeds for early SMBH formation (Blinnikov+'16; cf. recent JWST results on early galaxies at z~12)

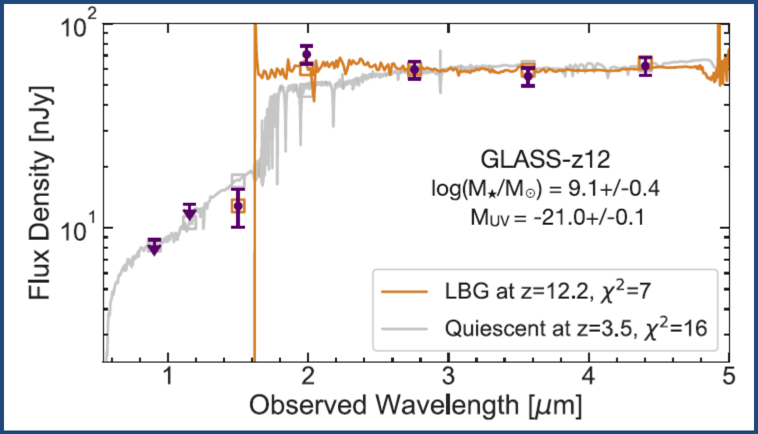

Naidu+'22

Binary NS and multimessenger astronomy

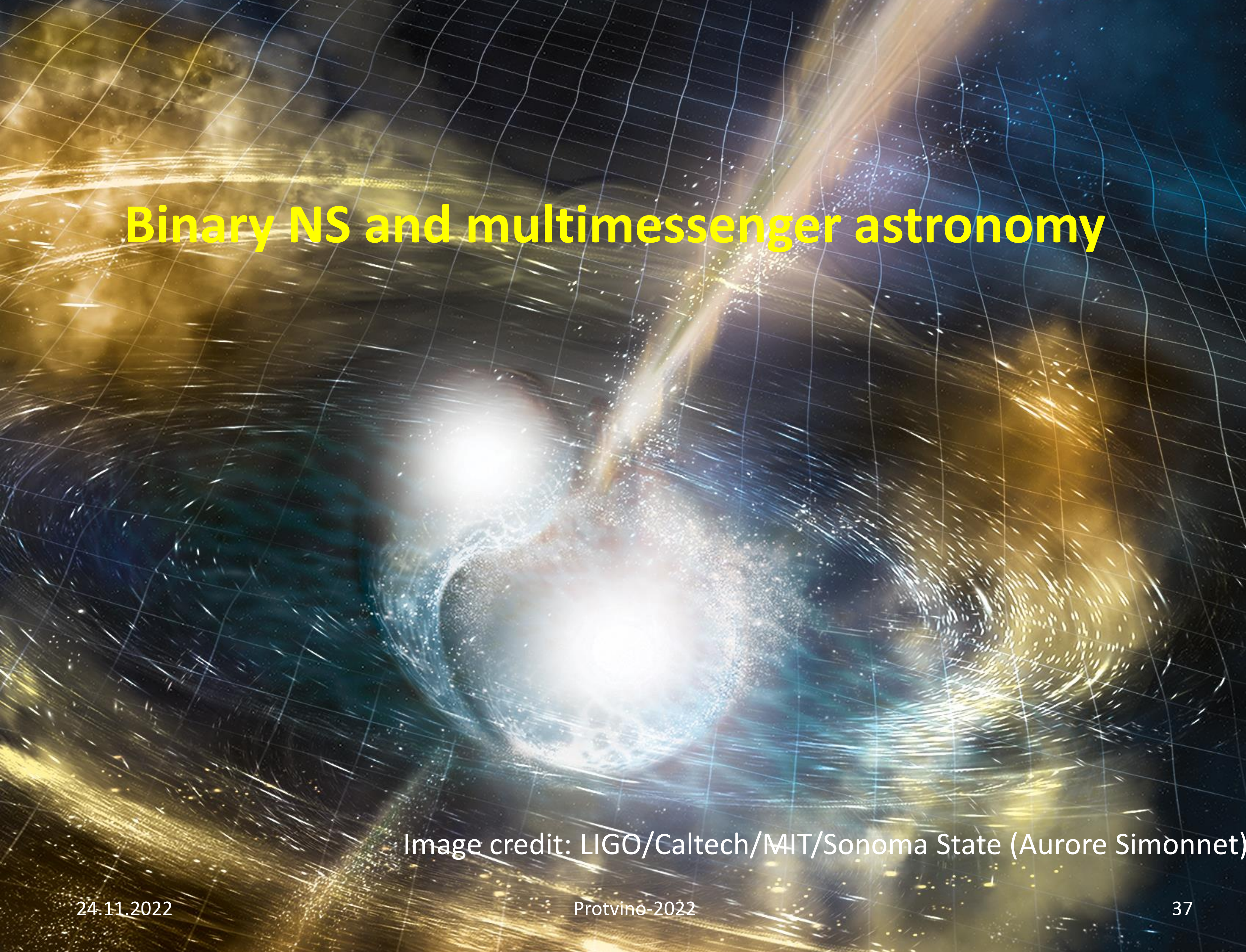

Image credit: LIGO/Caltech/MIT/Sonoma State (Aurore Simonnet)

GRB170817A and GW170817

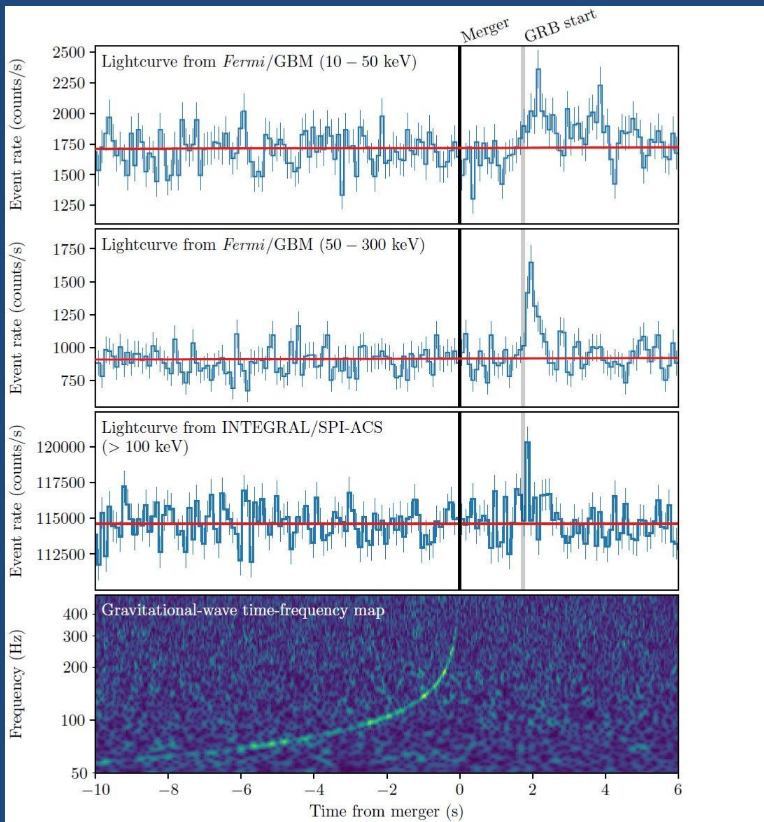

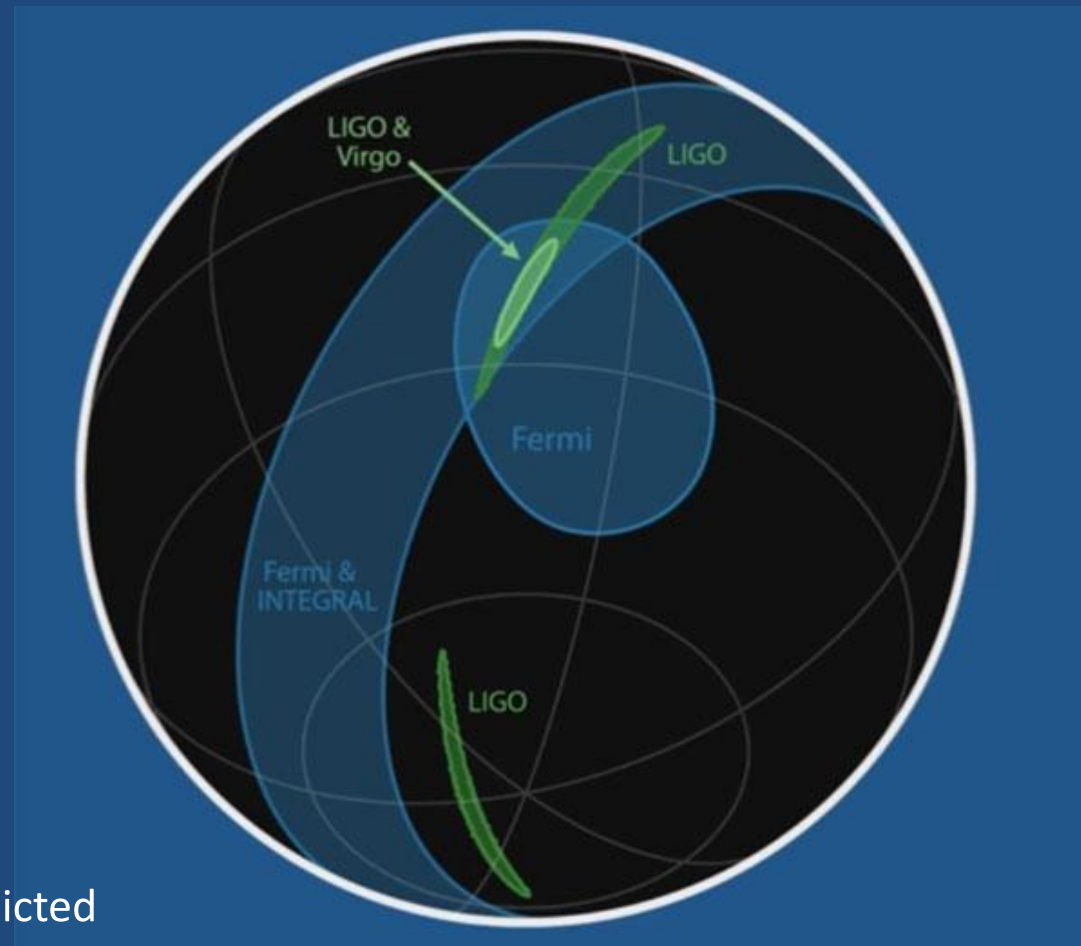

GRB association with NS+NS was predicted by Blinnikov et al. 1984 SvAL

$$L_{\rm iso} = (1.6 \pm 0.6) \times 10^{47}\ {\rm erg\ s^{-1}}$$

Fundamental inferences

- 1) EM and GW speed: $\Delta v / v_{\mathrm{EM}} \approx v_{\mathrm{EM}} \Delta t / D$

10-s EM delay $$-3 \times 10^{-15} \leqslant \frac{\Delta v}{v_{\mathrm{EM}}} \leqslant +7 \times 10^{-16}$$ Instantaneous, D>26 Mpc

- 2) Equivalence principle

Shapiro delay $$\delta t_{\mathrm{S}} = -\frac{1+\gamma}{c^3} \int_{r_e}^{r_o} U(\boldsymbol{r}(l))\, dl$$

MW: M=2.5x10^{11}M$_\odot$
R<100 kpc

$$-2.6 \times 10^{-7} \leqslant \gamma_{\mathrm{GW}} - \gamma_{\mathrm{EM}} \leqslant 1.2 \times 10^{-6}$$

Cf. from Cassini mission: 2.1+/-2.3 x 10^{-5}

ApJL, 848, L13, 2017

• 3) Number of additional dimensions

$$h \propto \frac{1}{d_L^{\gamma}}$$

$$\gamma = \frac{D-2}{2}$$

H_0 prior km s^{-1} Mpc^{-1}	γ	D
$H_0 = 73.24 \pm 1.74$ [22]	$1.01^{+0.04}_{-0.05}$	$4.02^{+0.07}_{-0.10}$
$H_0 = 67.74 \pm 0.46$ [21]	$0.99^{+0.03}_{-0.05}$	$3.98^{+0.07}_{-0.09}$

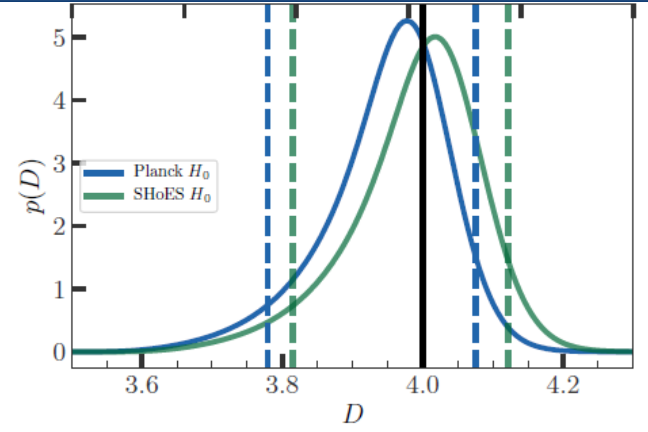

FIG. 1. Posterior probability distribution for the number of spacetime dimensions, D, using the GW distance posterior to GW170817 and the measured Hubble velocity to its host galaxy, NGC 4993, assuming the H_0 measurements from [21] (blue curve) and [22] (green curve). The dotted lines show

arXiv:1801.08160

Parameters from GW signal

	Low-spin priors ($\lvert\chi\rvert \leq 0.05$)	High-spin priors ($\lvert\chi\rvert \leq 0.89$)
Primary mass m_1	1.36–$1.60\ M_\odot$	1.36–$2.26\ M_\odot$
Secondary mass m_2	1.17–$1.36\ M_\odot$	0.86–$1.36\ M_\odot$
Chirp mass $\mathcal{M}$	$1.188^{+0.004}_{-0.002} M_\odot$	$1.188^{+0.004}_{-0.002} M_\odot$
Mass ratio m_2/m_1	0.7–1.0	0.4–1.0
Total mass $m_{\rm tot}$	$2.74^{+0.04}_{-0.01} M_\odot$	$2.82^{+0.47}_{-0.09} M_\odot$
Radiated energy $E_{\rm rad}$	$> 0.025 M_\odot c^2$	$> 0.025 M_\odot c^2$
Luminosity distance $D_{\rm L}$	40^{+8}_{-14} Mpc	40^{+8}_{-14} Mpc
Viewing angle Θ	$\leq 55°$	$\leq 56°$
Using NGC 4993 location	$\leq 28°$	$\leq 28°$
Combined dimensionless tidal deformability $\tilde{\Lambda}$	≤ 800	≤ 700
Dimensionless tidal deformability $\Lambda(1.4 M_\odot)$	≤ 800	≤ 1400

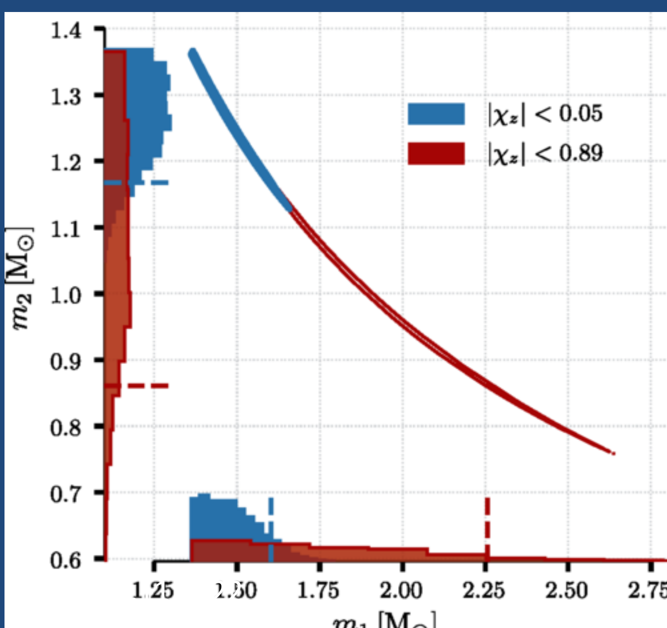

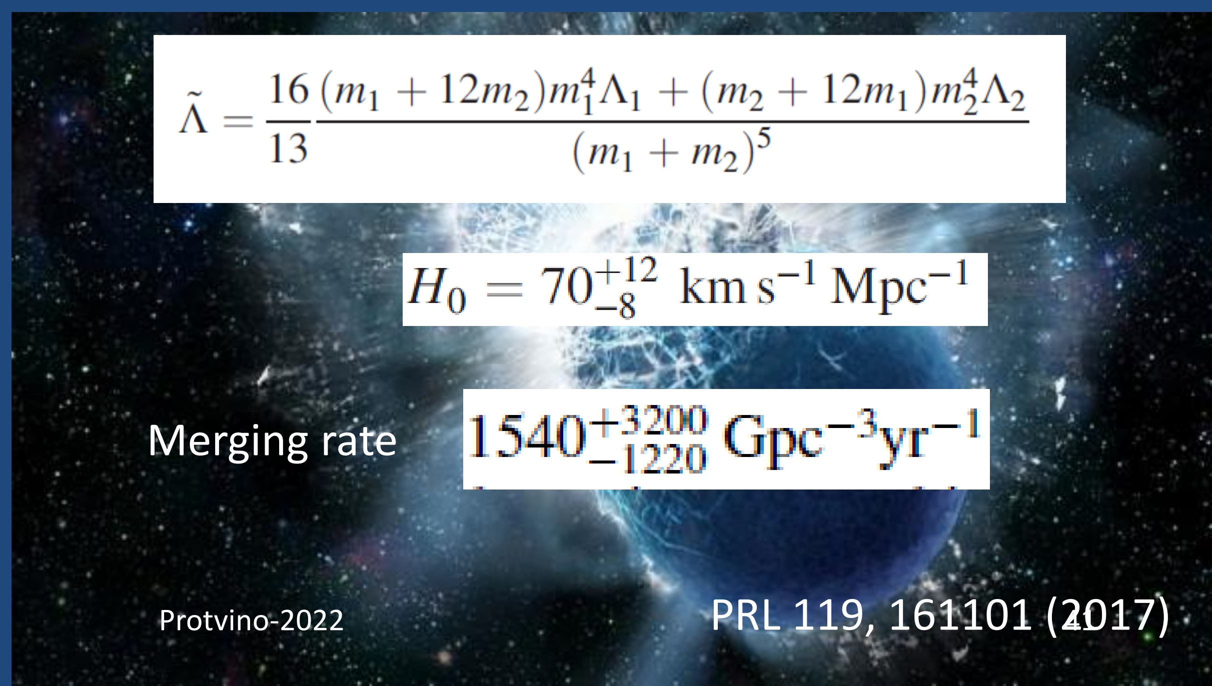

$$\tilde{\Lambda} = \frac{16}{13} \frac{(m_1 + 12 m_2) m_1^4 \Lambda_1 + (m_2 + 12 m_1) m_2^4 \Lambda_2}{(m_1 + m_2)^5}$$

$$H_0 = 70^{+12}_{-8}\ \mathrm{km\,s^{-1}\,Mpc^{-1}}$$

Merging rate $1540^{+3200}_{-1220}\ \mathrm{Gpc^{-3}yr^{-1}}$

PRL 119, 161101 (2017)

Optical and IR observations of kilonova

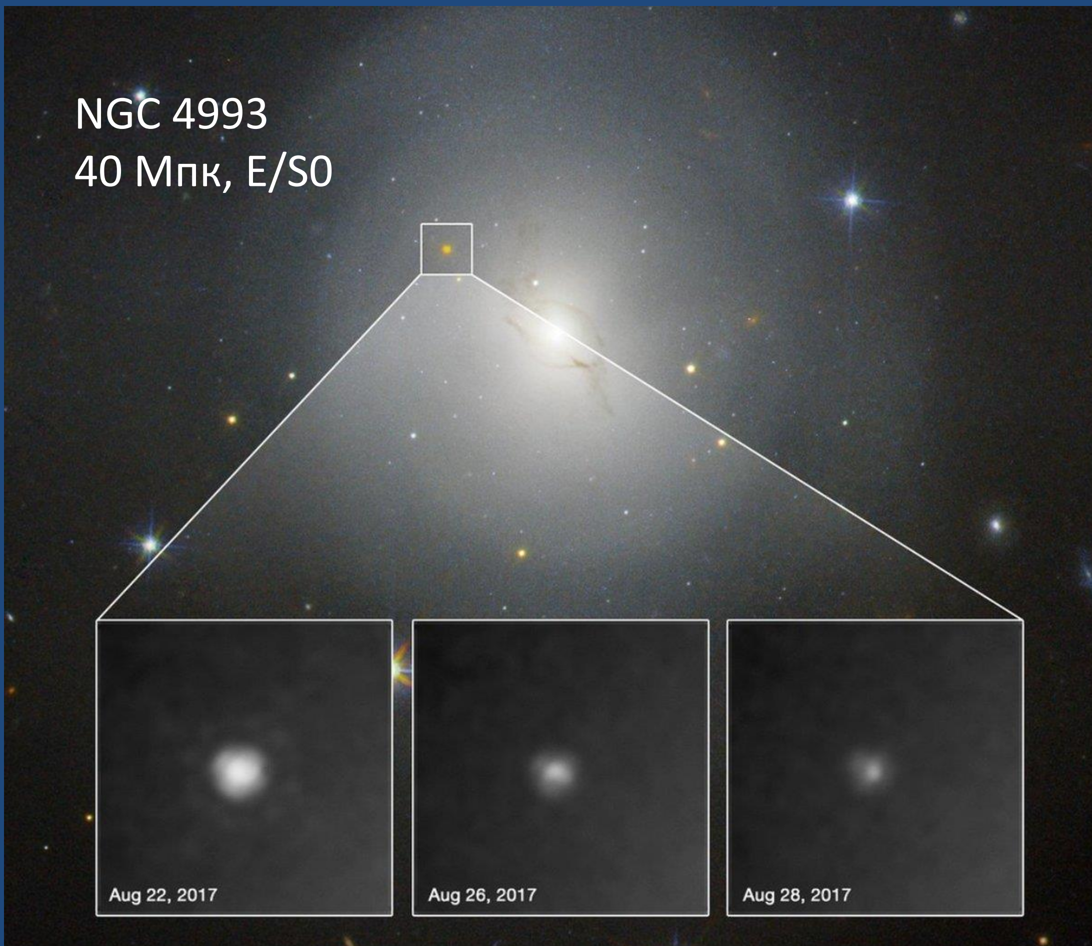

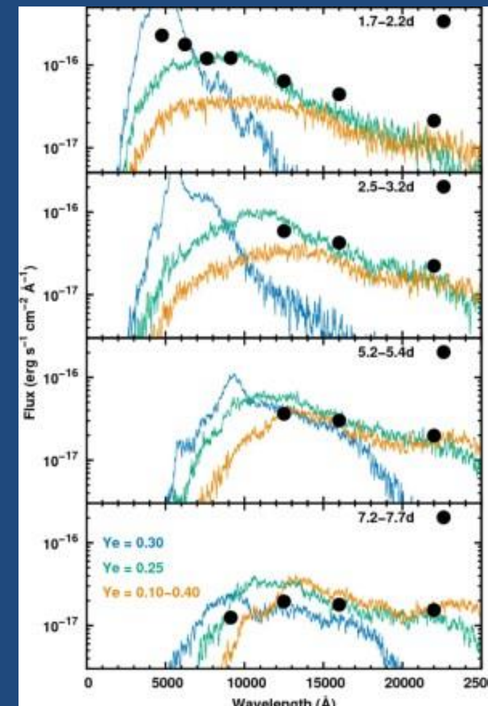

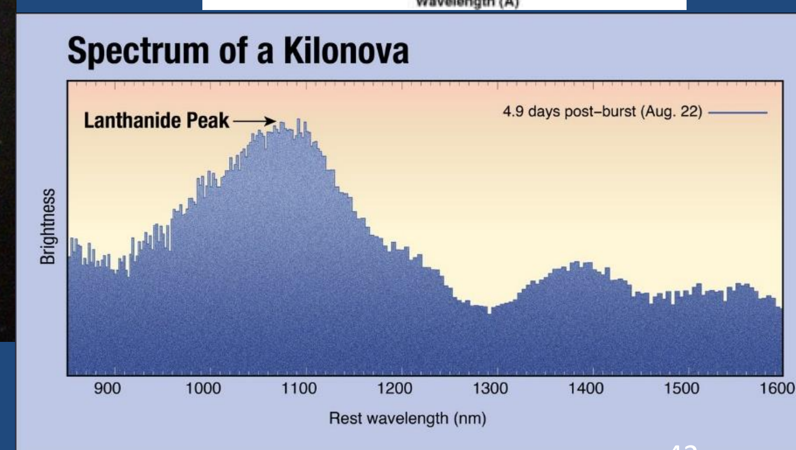

1710.05850

Binary NS as main production channel for r-elements

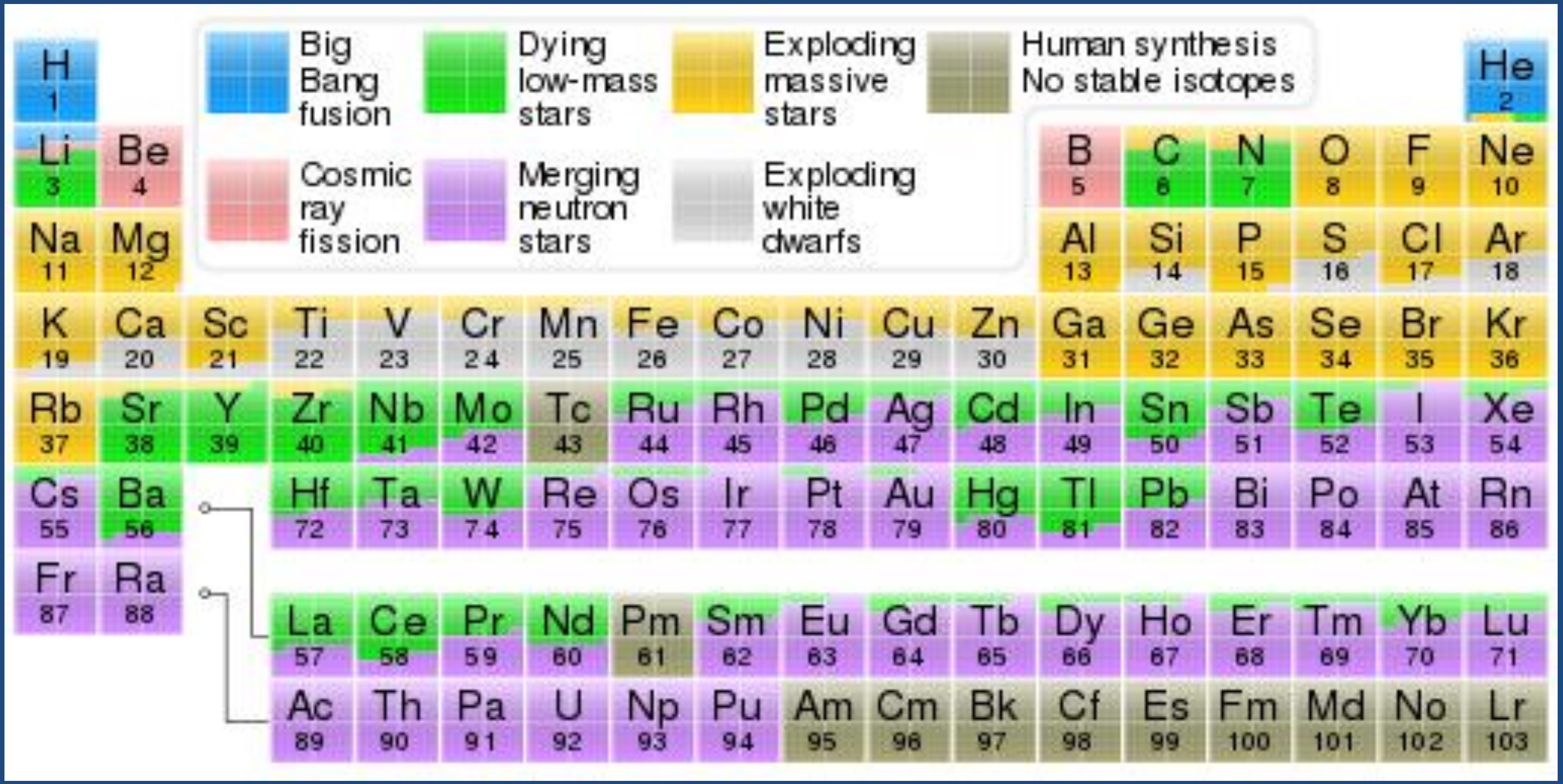

Joint GW+kilonova analysis

Table 1: Key Properties of GW170817

Property	Value	Reference
Chirp mass, $\mathcal{M}$ (rest frame)	$1.188^{+0.004}_{-0.002} M_\odot$	1
First NS mass, M_1	$1.36 - 1.60 M_\odot$ (90%, low spin prior)	1
Second NS mass, M_2	$1.17 - 1.36 M_\odot$ (90%, low spin prior)	1
Total binary mass, $M_{\rm tot} = M_1 + M_2$	$\approx 2.74^{0.04}_{-0.01} M_\odot$	1
Observer angle relative to binary axis, $\theta_{\rm obs}$	$11 - 33^\circ$ (68.3%)	2
Blue KN ejecta ($A_{\rm max} \lesssim 140$)	$\approx 0.01 - 0.02 M_\odot$	e.g., 3,4,5
Red KN ejecta ($A_{\rm max} \gtrsim 140$)	$\approx 0.04 M_\odot$	e.g., 3,5,6
Light r-process yield ($A \lesssim 140$)	$\approx 0.05 - 0.06 M_\odot$	
Heavy r-process yield ($A \gtrsim 140$)	$\approx 0.01 M_\odot$	
Gold yield	$\sim 100 - 200 M_\oplus$	8
Uranium yield	$\sim 30 - 60 M_\oplus$	8
Kinetic energy of off-axis GRB jet	$10^{49} - 10^{50}$ erg	e.g., 9, 10, 11, 12
ISM density	$10^{-4} - 10^{-2}$ cm^{-3}	e.g., 9, 10, 11, 12

(1) LIGO Scientific Collaboration et al. 2017c; (2) depends on Hubble Constant, LIGO Scientific Collaboration et al. 2017d; (3) Cowperthwaite et al. 2017; (4) Nicholl et al. 2017; (5) Kasen et al. 2017; (6) Chornock et al. 2017; (8) assuming heavy r-process ($A > 140$) yields distributed as solar abundances (Arnould et al., 2007); (9)Margutti et al. 2017; (10) Troja et al. 2017; (11) Fong et al. 2017; (12) Hallinan et al. 2017

B.Metzger 1710.05931

Cosmological inferences

- 1) Independent "standard siren" measurement of H_0 from binary NS mergings
- GW170817: $H_0 = 70^{+12}_{-8}\ km\ s^{-1}\ Mpc^{-1}$ [Abbott+'17]
- $H_0 = 72^{+12}_{-8}\ km\ s^{-1}\ Mpc^{-1}$ [Palmese+'20]

- 2) Indication of the existence of massive primordial black holes from binary BH mergings [Blinnikov+'16,Dolgov+'20,...]

Future prospects (LVK collaboration)

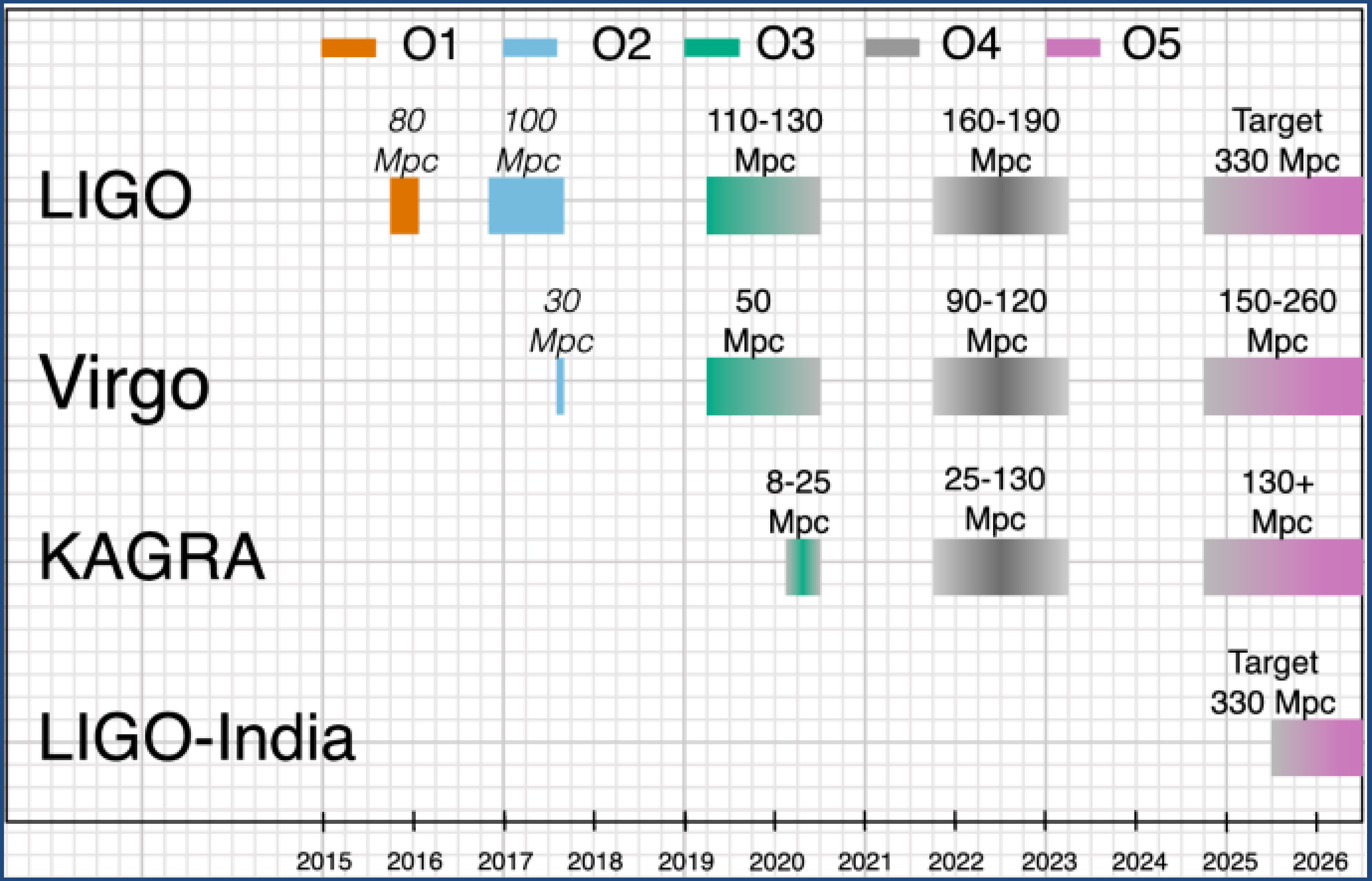

Abbot et al. 2020

40-km LIGO Cosmic Explorer (2035)

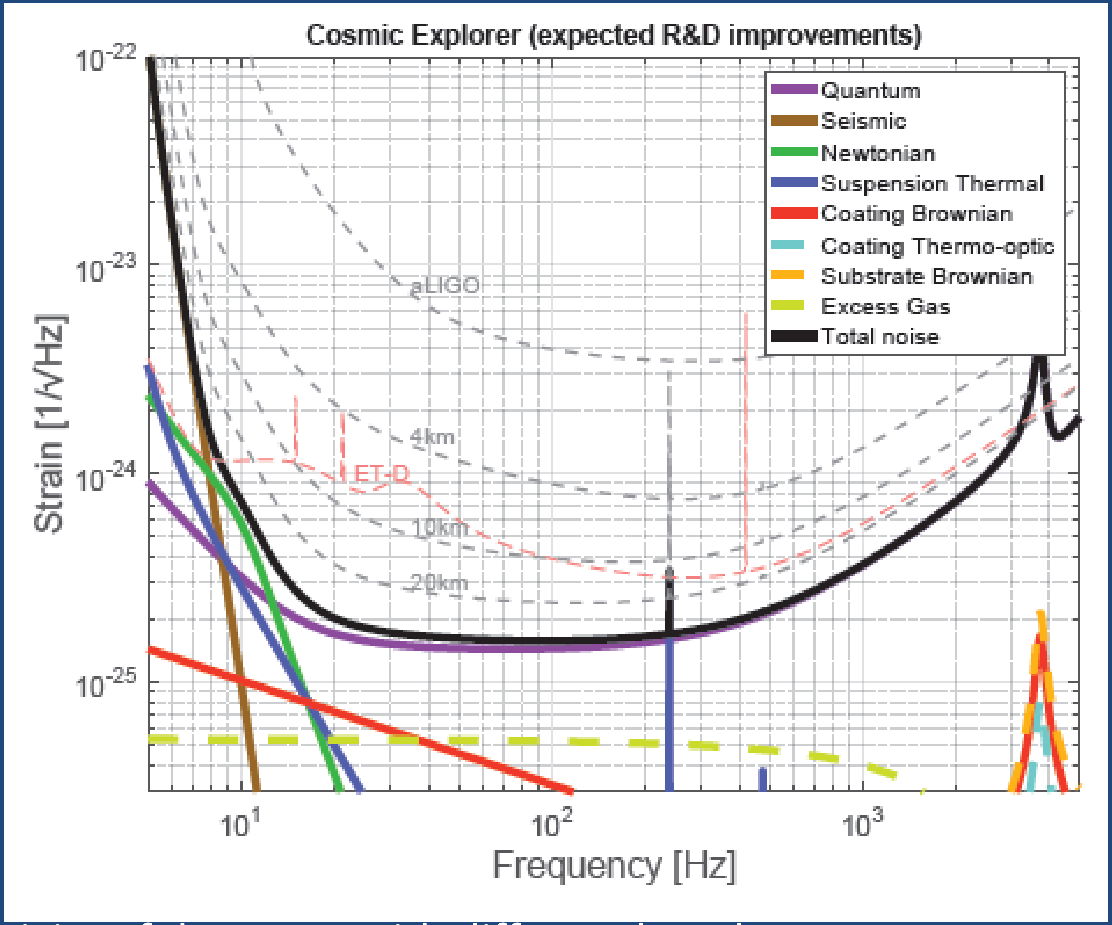

Sensitivity of detectors with different lengths.
Solid curves are for a 40km long detector

LIGO Scientific Collaboration,arXiv:1607.08697 [astro-ph.IM]

- LIGO, Virgo, and KAGRA are closely coordinating to start the O4 Observing run together in ~**March 2023**, despite local and global adversities.
- LIGO projects a sensitivity goal of 160-190 Mpc for binary neutron stars. Virgo projects a target sensitivity of 80-115 Mpc. KAGRA should be running with greater than 1 Mpc sensitivity at the beginning of O4, and will work to improve the sensitivity toward the end of O4.

Pulsar timing arrays (PTA)

- Pulsar timing (Estabrook & Walquist'75, Sazhin'78, Detweiler'79)
- Working collaborations
  - European PTA (EPTA) [42 msPSR]
  - Indian PTA (In PTA)
  - North American Nanohertz Observatory for GW (NANOGrav) [48 msPSR]
  - Parkes PTA (PPTA) [~30 msPSR]
  - >Join into International PTA (IPTA)

$R(ns) \sim 10\,(h/10^{-16})/\,(f/10^{-8}\,Hz)$

NanoHz GW from PTA observations

- Stochastic GW backgrounds: $h_c = A(f/1\,\mathrm{yr}^{-1})^{\alpha}$
  - Inspiral binary SMBH (M>10^7) (e.g. Sesana+'08, α=-2/3)
  - Cosmic strings (e.g. Oelmez+'10, α=-7/6)
  - Cosmological phase transitions, primordial GW (Grishchuk'05 α=-2, Lasky+'16 α=-1)
  - …

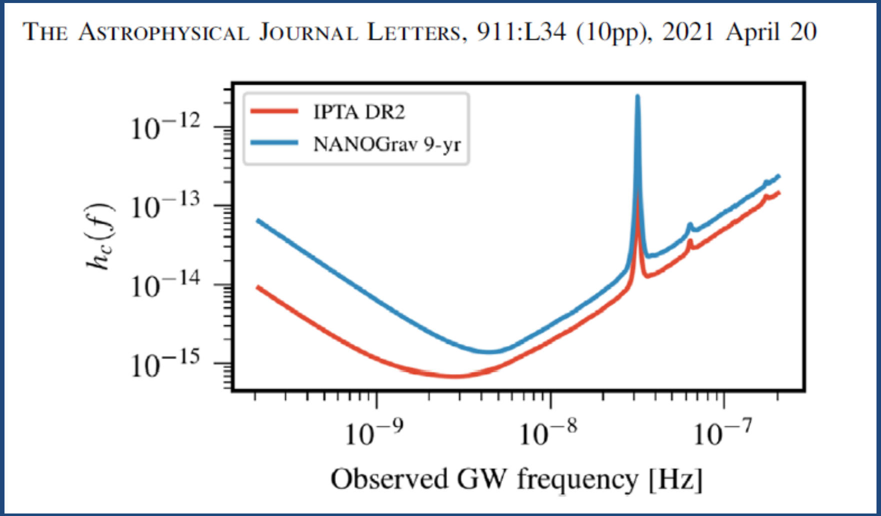

Pol+'21

IPTA DR2 results

$$h_c(f) = A_{\rm CP}\left(\frac{f}{f_{\rm yr}}\right)^{(3-\gamma_{\rm CP})/2}$$

- Stochastic common spectrum process (CP)

$$h_c = A(f/1\,{\rm yr}^{-1})^{\alpha}$$
$$A = 3.8^{+6.3}_{-2.5}\times 10^{-15}$$
$$\alpha = -0.5 \pm 0.5$$

- Marginally consistent with SMBH GWB (α=-2/3) with space density

$$\Phi_0 \approx 10^{-5}{\rm Mpc}^{-3}$$

- Cosmic string tension μG~[4-10]x10^{-11} (Ellis,Lewicki’21)

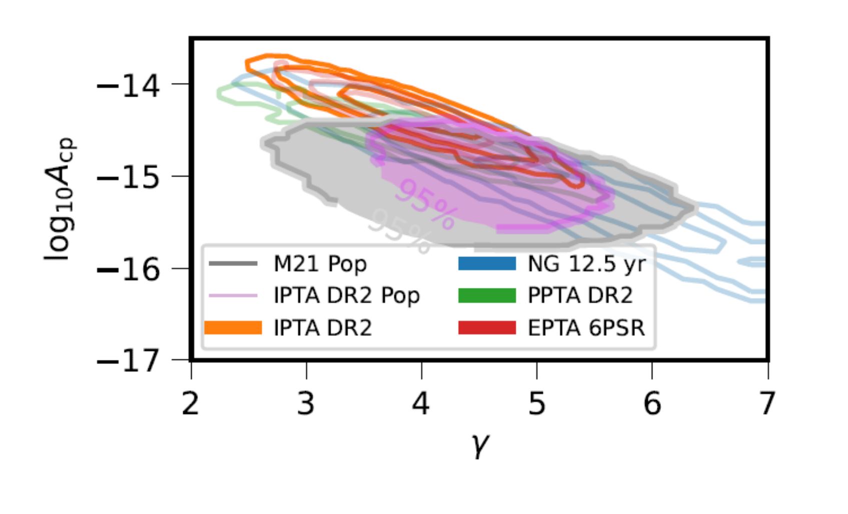

$$A^2_{\rm GWB} = \frac{4}{3\pi^{1/3}}\iiint dM_1 dz dq \frac{\mathcal{M}^{5/3}}{(1+z)^{1/3}}\frac{d^3\Phi_{\rm BHB}}{dM_1 dz dq}$$

Antoniadis+ 2201.03980

Cosmological inferences if detected CP signal is GWB

- 2d-order GWs accompanying formation of PBH from collapse of inflationary scalar perturbations

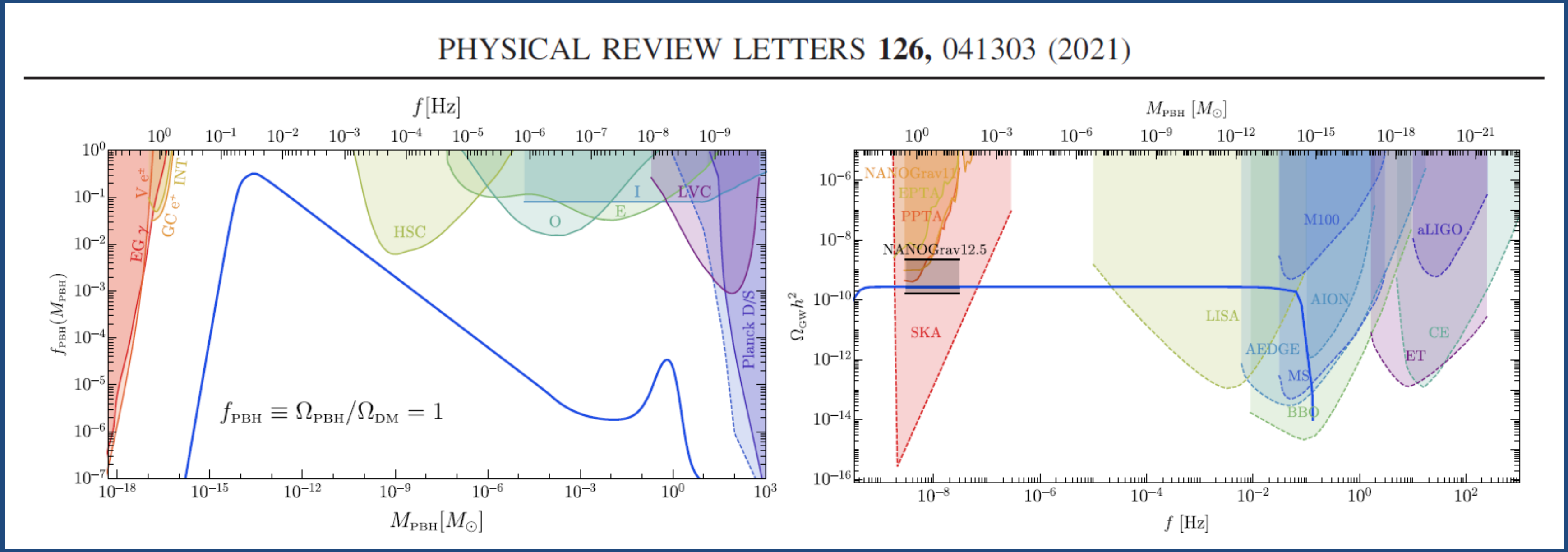

De Luca, Franciolini, Riotto ’21

Conclusions

- LVK O1+O2+O3: ~ 91 detections of binary BH and NS mergings, mostly binary BH, rate ~10-200 $Gpc^{-3}\ yr^{-1}$
- Astrophysical problems in formation of massive BH with $M \sim 100\ M_\odot$, extreme mass ratio BH+BH inspirals, BH+NS
- Stochastic nanoHz CP signal is detected by NANOGrav and IPTA collaborations. If GWB, it may be produced by SMBH binaries ~$10^{-5}\ Gpc^{-3}$
- Pulsar timing as a sensitive probe to new theoretical models of nanoHz GWBs!

Backup slides

How to measure tiny displacements?

$$\Delta\Phi = B\frac{hL}{\lambda}, \quad \frac{BL}{c} \le \frac{1}{2}\left(\frac{1}{f_{GW}}\right) \Rightarrow B_{\max} \approx 400$$

$$Shot\,noise: \;\; \Delta\Phi_{\min} \sim \frac{1}{\sqrt{N_{ph}}},$$

$$N_{ph} = \frac{P_{laser} \times (\#\ recyclings)}{\hbar\omega} \times \Delta t \sim 2\times 10^{20}$$

$$@\,P = 60W, \;\; \Delta t = 10ms$$

$$h_{\min} \sim \frac{\lambda}{BL}\frac{1}{\sqrt{N_{ph}}} = \frac{0.5\mu}{400\times 4km}\frac{1}{\sqrt{2\times 10^{20}}} \sim 10^{-22}\,!$$

Hellings-Downes correlation

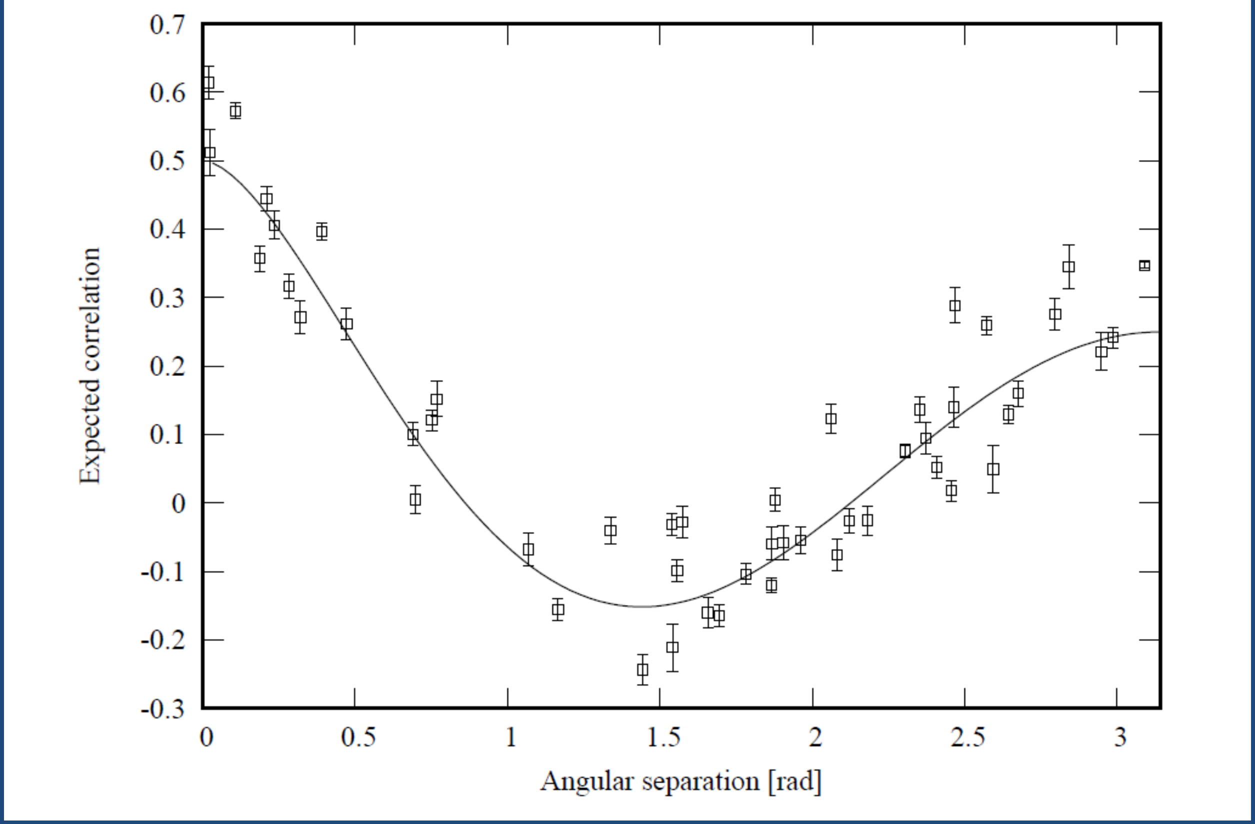

$$\langle r_a^*(t) r_b(t)\rangle = 2C(\xi)\int_0^\infty df\, \frac{S_h(f)}{(2\pi f)^2} 2[1-\cos(2\pi t)]$$

$$C(\xi) = \frac{1}{3}\left\{1 + \frac{3}{2}(1-\cos\xi)\left[\ln\left(\frac{1-\cos\xi}{2}\right) - \frac{1}{6}\right]\right\}$$

- GR spin-orbital precession
- High BH spin…

NSBH mergers

- GW 200105_1162426 (8.9+1.9)

- GW 299115_042309 (5.4+1.5) $\chi_{\rm eff} = -0.19^{+0.23}_{-0.35}$??

Predictions from binary star evolution

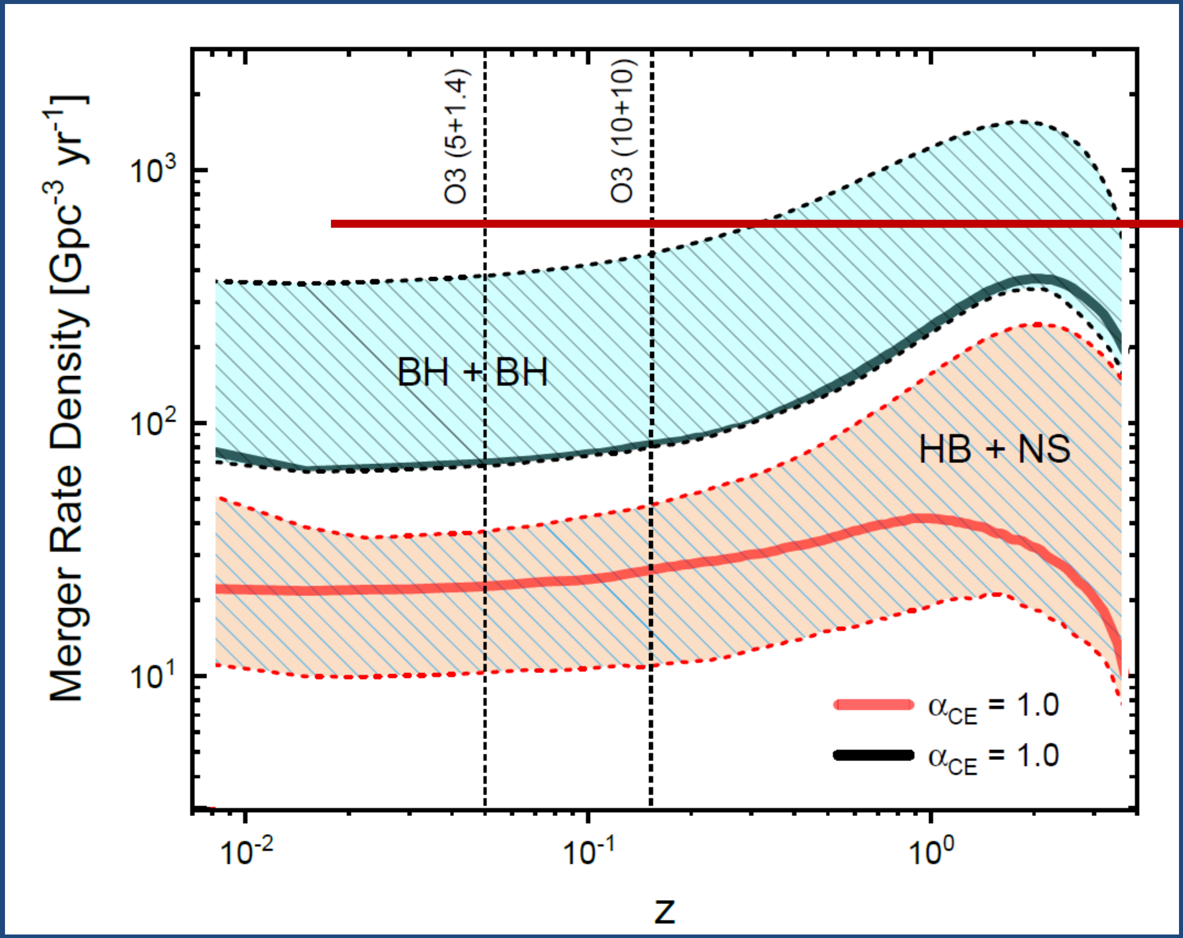

NS+BH upper limit
610 Gpc^{-3} yr^{-1}

1811.12907

PK+ 2019; 1907.04218

Detection rate BH+BH, BH+NS

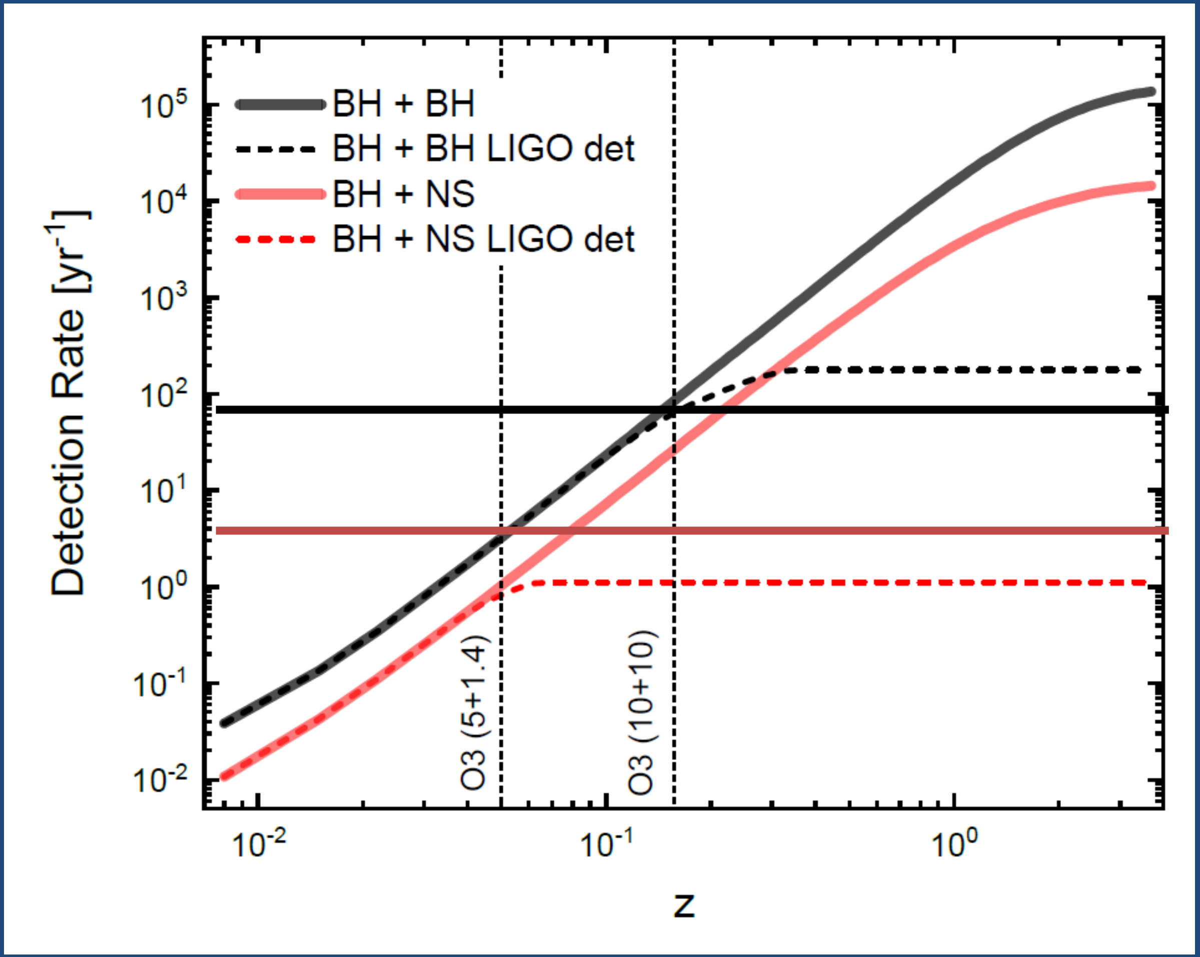

Actual detections

1907.04218

EM emission from NS+BH

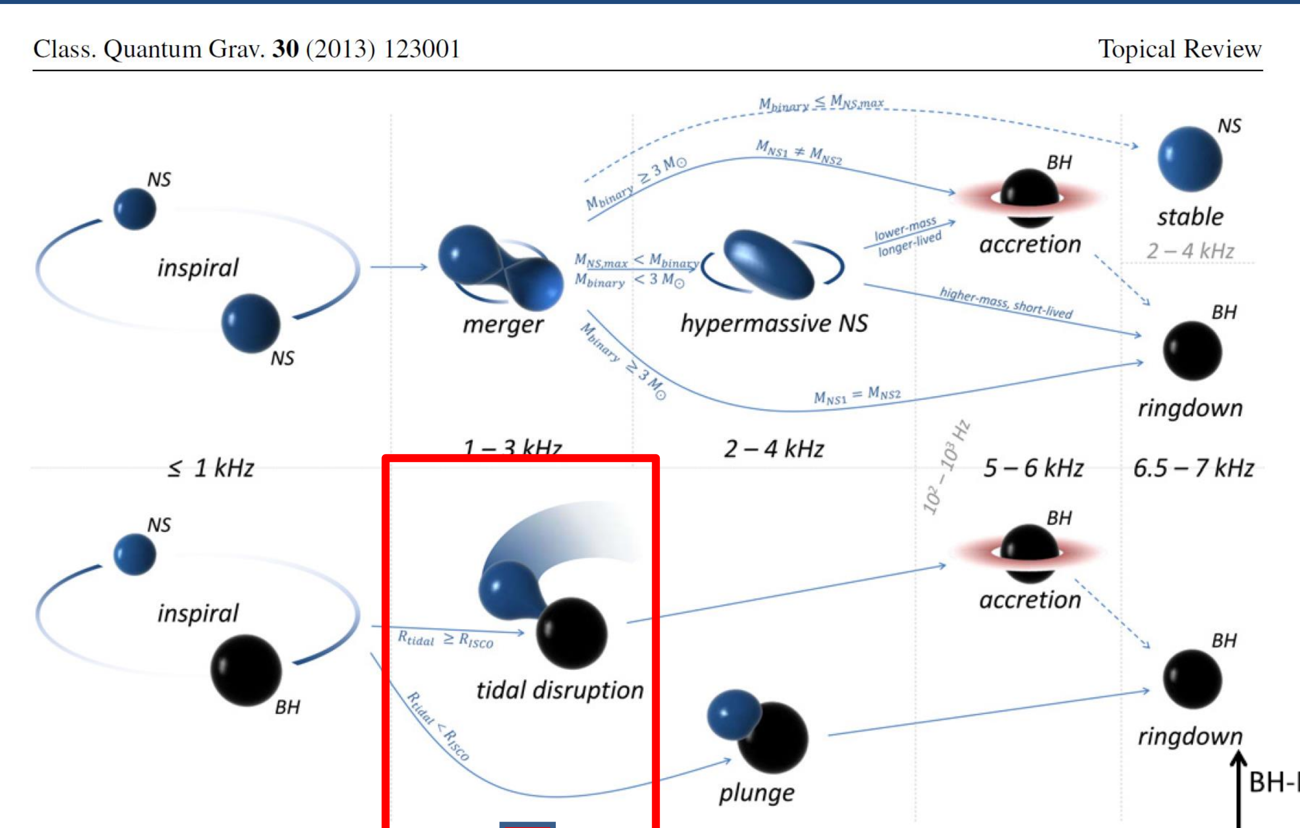

EM-favorable

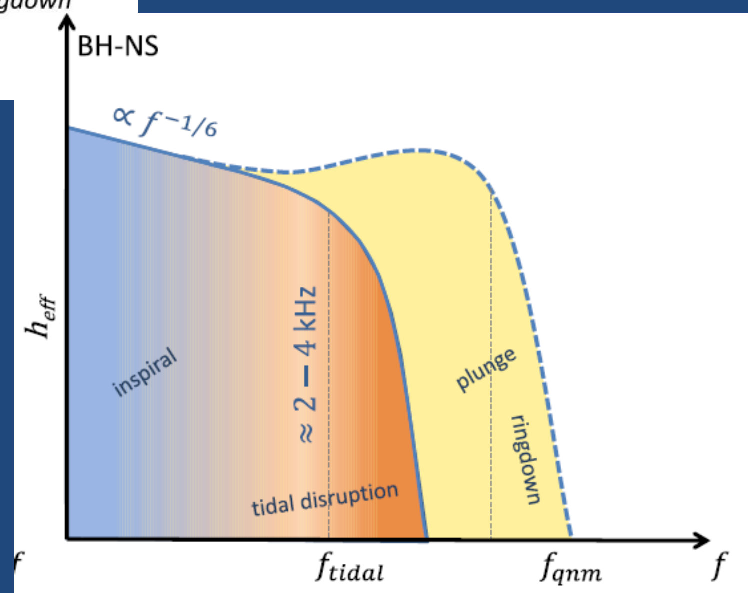

Mass shedding and tidal disruption

$$r_{\rm ISCO}/M = 3 + Z_2 \mp \sqrt{(3 - Z_1)(3 + Z_1 + 2Z_2)}$$
$$Z_1 \equiv 1 + (1 - \chi_1^2)^{1/3} \times \left[(1 + \chi_1)^{1/3} + (1 - \chi_1)^{1/3}\right]$$
$$Z_2 \equiv \sqrt{3\chi_1^2 + Z_1^2}$$

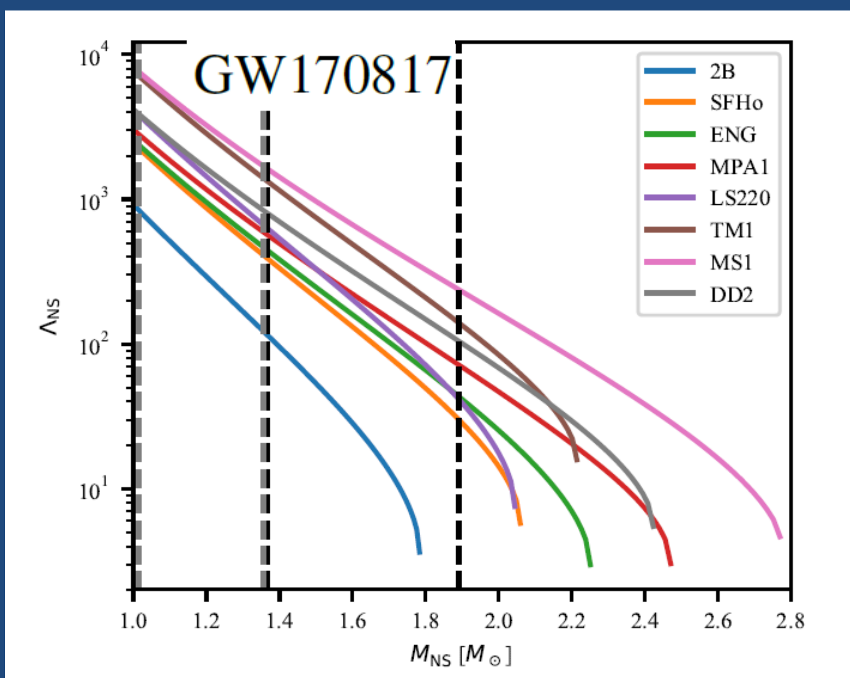

Barbieri+ 1908.08822

- $R_{tid} \sim R_{ns}(M_{bh}/M_{ns})^{1/3}$
  Mass shedding if
  $R_{tid} > R_{ISCO}$
- Depends on NS compactness $C = M_{ns}/R_{ns}$ (EOS)
- **Tidal parameter $\Lambda = 2k_2/(3C^5)$**
- Depends on the BH spin